

# Journal Pre-proof

Physicochemical parameters data assimilation for efficient improvement of water quality index prediction: Comparative assessment of a noise suppression hybridization approach

Mohammad Rezaie-Balf, Nasrin Fathollahzadeh Attar, Ardashir Mohammadzadeh, Muhammad Ary Murti, Ali Najah Ahmed, Chow Ming Fai, Narjes Nabipour, Sina Alaghmand, Ahmed El-Shafie

PII: S0959-6526(20)32623-8

DOI: <https://doi.org/10.1016/j.jclepro.2020.122576>

Reference: JCLP 122576

To appear in: *Journal of Cleaner Production*

Received Date: 30 November 2019

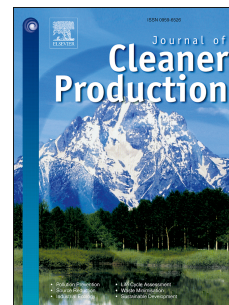
Revised Date: 12 May 2020

Accepted Date: 27 May 2020

Please cite this article as: Rezaie-Balf M, Attar NF, Mohammadzadeh A, Murti MA, Ahmed AN, Fai CM, Nabipour N, Alaghmand S, El-Shafie A, Physicochemical parameters data assimilation for efficient improvement of water quality index prediction: Comparative assessment of a noise suppression hybridization approach, *Journal of Cleaner Production*, <https://doi.org/10.1016/j.jclepro.2020.122576>.

This is a PDF file of an article that has undergone enhancements after acceptance, such as the addition of a cover page and metadata, and formatting for readability, but it is not yet the definitive version of record. This version will undergo additional copyediting, typesetting and review before it is published in its final form, but we are providing this version to give early visibility of the article. Please note that, during the production process, errors may be discovered which could affect the content, and all legal disclaimers that apply to the journal pertain.

© 2020 Elsevier Ltd. All rights reserved.



1 **Physicochemical parameters data assimilation for efficient improvement of**  
2 **water quality index prediction: Comparative assessment of a noise**  
3 **suppression hybridization approach**

4  
5 Mohammad Rezaie-Balf<sup>1</sup>, Nasrin Fathollahzadeh Attar<sup>2</sup>, Ardashir Mohammadzadeh<sup>3</sup>,  
6 Muhammad Ary Murti<sup>4</sup>, Ali Najah Ahmed<sup>5</sup>, Chow Ming Fai<sup>6</sup>, Narjes Nabipour<sup>7</sup>, Sina  
7 Alaghmand<sup>8</sup>, Ahmed El-Shafie<sup>9,10</sup>

8  
9  
10 <sup>1</sup>*Department of Water Engineering, Graduate University of Advanced Technology, Kerman,*  
11 *Iran. Email: moe.rezaie69@gmail.com*

12 <sup>2</sup>*Water Engineering Department, Urmia University, Urmia, Iran.*  
13 *Email: n.fatolahzadeh@urmia.ac.ir*

14 <sup>3</sup>*Department of electrical engineering, Faculty of Engineering University of Bonab, Bonab, Iran.*  
15 *Email: a.mzadeh@bonabu.ac.ir*

16 <sup>4</sup>*Research Center for IoT, Telkom University, Bandung 40257, Indonesia.*  
17 *Email: Arymurti@telkomuniversity.ac.id*

18 <sup>5</sup>*Institute of Energy Infrastructure (IEI), Universiti Tenaga Nasional (UNITEN), 43000*  
19 *Selangor, Malaysia. Email: Mahfoodh@uniten.edu.my*

20 <sup>6</sup>*Institute of Sustainable Energy (ISE), Universiti Tenaga Nasional, Kajang 43000, Selangor,*  
21 *Malaysia. Email: Chowmf@uniten.edu.my*

22 <sup>7</sup>*Institute of Research and Development, Duy Tan University, Da Nang 550000, Viet Nam.*  
23 *Email: narjesnabipour@duytan.edu.vn.*

24 <sup>8</sup>*Department of Civil Engineering, Monash University, 23 College Walk, Clayton, VIC 3800,*  
25 *Australia. Email: Sina.Alaghmand@monash.edu*

26 <sup>9</sup>*Department of Civil Engineering, University of Malaya, Kuala Lumpur, 50603, Malaysia.*  
27 *Email: elshafie@um.edu.my*

28 <sup>10</sup>*National Water Center, United Arab Emirates University, Al Ain, United Arab Emirates*

29  
30  
31 **Corresponding Author: Mohammad Rezaie-Balf**

32 **Email: moe.rezaie69@gmail.com**

1 **Physicochemical parameters data assimilation for efficient improvement of**  
2 **water quality index prediction: Comparative assessment of a noise**  
3 **suppression hybridization approach**

4  
5 Mohammad Rezaie-Balf<sup>1</sup>, Nasrin Fathollahzadeh Attar<sup>2</sup>, Ardashir Mohammadzadeh<sup>3</sup>,  
6 Muhammad Ary Murti<sup>4</sup>, Ali Najah Ahmed<sup>5</sup>, Chow Ming Fai<sup>6</sup>, Narjes Nabipour<sup>7</sup>, Sina  
7 Alaghmand<sup>8</sup>, Ahmed El-Shafie<sup>9,10</sup>

8  
9  
10 <sup>1</sup>*Department of Water Engineering, Graduate University of Advanced Technology, Kerman,*  
11 *Iran. Email: moe.rezaie69@gmail.com*

12 <sup>2</sup>*Water Engineering Department, Urmia University, Urmia, Iran.*  
13 *Email: n.fatolahzadeh@urmia.ac.ir*

14 <sup>3</sup>*Department of electrical engineering, Faculty of Engineering University of Bonab, Bonab, Iran.*  
15 *Email: a.mzadeh@bonabu.ac.ir*

16 <sup>4</sup>*Research Center for IoT, Telkom University, Bandung 40257, Indonesia.*  
17 *Email: Arymurti@telkomuniversity.ac.id*

18 <sup>5</sup>*Institute of Energy Infrastructure (IEI), Universiti Tenaga Nasional (UNITEN), 43000*  
19 *Selangor, Malaysia. Email: Mahfoodh@uniten.edu.my*

20 <sup>6</sup>*Institute of Sustainable Energy (ISE), Universiti Tenaga Nasional, Kajang 43000, Selangor,*  
21 *Malaysia. Email: Chowmf@uniten.edu.my*

22 <sup>7</sup>*Institute of Research and Development, Duy Tan University, Da Nang 550000, Viet Nam.*  
23 *Email: narjesnabipour@duytan.edu.vn.*

24 <sup>8</sup>*Department of Civil Engineering, Monash University, 23 College Walk, Clayton, VIC 3800,*  
25 *Australia. Email: Sina.Alaghmand@monash.edu*

26 <sup>9</sup>*Department of Civil Engineering, University of Malaya, Kuala Lumpur, 50603, Malaysia.*  
27 *Email: elshafie@um.edu.my*

28 <sup>10</sup>*National Water Center, United Arab Emirates University, Al Ain, United Arab Emirates*

29  
30  
31 **Corresponding Author: Mohammad Rezaie-Balf**

32 **Email: moe.rezaie69@gmail.com**

33

34

## 35 **Abstract**

36 Water quality has a crucial impact on human health; therefore, water quality index modeling is  
37 one of the challenging issues in the water sector. The accurate prediction of water quality index  
38 is an essential requisite for water quality management, human health, public consumption, and  
39 domestic uses. A comprehensive review as an initial attempt is conducted on existing solutions  
40 through data-driven models. In addition, the ensemble Kalman filter is found to be a suitable  
41 data assimilation method, which is successfully applied in hydrological variables modeling and  
42 other complexes, nonlinear, and chaotic problems. In this study, a new application of ensemble  
43 Kalman filter-artificial neural network is proposed to predict water quality index using  
44 physicochemical parameters for two commonly pollutant rivers, namely Klang and Langat, in  
45 Malaysia. As a further attempt, in order to improve the models' performance, a new  
46 preprocessing technique is adopted as the newly constructed assimilated model. The results  
47 confirm that ensemble hybrid based intrinsic time-scale decomposition has reduced root mean  
48 square error by 24 % for Klang and 34 % for Langat, respectively, compared with the intrinsic  
49 time-scale decomposition-conventional neural network model. Overall, the developed  
50 assimilated methodology shows the robustness of the proposed ensemble hybrid model in  
51 analyzing water quality index over monthly horizons that experts could evaluate the water  
52 quality of rivers more efficiently.

53

54 **Keywords:** Physicochemical Parameters, Water Quality Index, Data Assimilation, Ensemble  
55 Kalman Filter, Intrinsic Time-scale Decomposition.

56

57

58

59

60 **Nomenclature**

61	ALK= Alkalinity	AN= Ammoniacal-Nitrate
62	ANFIS=Adaptive Neuro-Fuzzy Inference System	ANN= Artificial Neural Network
63	ANOVA= One-Way Analysis of Variance	As=Arsenic
64	Atr= Atrazine	BOD= Biological Oxygen Demand
65	BTEX= Benzene–Toluene–Ethylbenzene–Xylenes	C=Coliform
66	Ca= Calcium	CA= Cluster Analysis
67	Cd= Cadmium	COD= Chemical Oxygen Demand
68	Cl= Chlorine	Cr= Chromium
69	Cu= Copper	DA= Data Assimilation
70	DO= Dissolved Oxygen	DoE= Department of Environment
71	DDMs= Data-Driven Models	DS= Dissolved Solids
72	DT=Decision Tree	EC= Electrical Conductivity
73	EnKF= Ensemble Kalman Filter	F= Fluorides
74	FC=Faecal Coliforms	Fe= Iron
75	FS=Fourier Series	FST= Faecal Streptococcus
76	GA=Genetic Algorithm	GD= Gradient Descent
77	HCA=Hierarchical Cluster Analysis	HCBD= HexaChlorButaDiene
78	Hg= Mercury	ITD= intrinsic time-scale decomposition
79	K=Potassium	KNN= K-Nearest Neighbor
80	LS-SVM=Least Square-Support Vector Machine	MAE= Mean Absolute Error
81	Mg= Magnesium	MLR=Multiple Linear Regression
82	MNNs=Multiple Neural Networks	MSA= Multivariate Statistical Analyses
83	Na= Natrium	NB = Naive Bayes
84	NH <sub>3</sub> =Ammonia	NH <sub>3</sub> -N= Ammoniacal Nitrogen
85	NH <sub>4</sub> = Ammonia	NH <sub>4</sub> -N=Ammonia-Nitrogen
86	Ni= Nickel	NO <sub>2</sub> = Nitrite
87	NO <sub>2</sub> -N=Nitrite Nitrogen	NO <sub>3</sub> =Nitrate

88	NO <sub>3</sub> -N= Nitrate Nitrogen	NSE= Nash-Sutcliffe Efficiency
89	NTU= Turbidity	OG= Oil and Grease
90	PAH= Polycyclic Aromatic Hydrocarbons	Pb= Plumbum
91	pH= Potential Hydrogen	PO <sub>4</sub> =Phosphate
92	PO <sub>4</sub> -P= Phosphate Phosphorous	PRC= Proper Rotation Components
93	PSO =Particle Swarm Optimization	RBC=Rule-Based Classifier
94	RBFN= Radial Basis Function Network	RMSE= Root Mean Square Error
95	RSD= Ratio of RMSE to Standard Deviation	Sa= Salmonellas
96	Sim= Simazine	SMLR= Stepwise Multiple Linear Regressions
97	SO <sub>4</sub> = Sulphates	SS= Suspended Solid
98	SVR= Support Vector Regression	T= Temperature
99	TA- CaCO <sub>3</sub> = Total Alkalinity of Calcium Carbonate	TC= Total Coliforms
100	TCB= TriChloroBenzenes	TDS= Total Dissolved Solid
101	TH=Total Hardness	TH- CaCO <sub>3</sub> =Total Hardness of Calcium Carbonate
102	TP= Total Phosphorus	TOC= Total Organic Carbon
103	TS= Total Solids	TSS= Total Suspended Solids
104	Twater= Water Temperature	U95= Uncertainty at 95 %
105	WQI= Water Quality Index	Zn= Zinc
106		

## 107 **1. Introduction**

108 Water is the crucial natural element for human survival and social development as well as the  
 109 ecological (natural, biological, environmental) health (Li et al., 2009). Water is the fundamental  
 110 element for industrial, agriculture, and biotransformation purposes regardless of drinking and  
 111 personal hygiene. In the last few decades, water pollution has turned into a severe problem  
 112 worldwide, particularly in developing countries. Water quality evaluation is, therefore, an  
 113 essential issue since it directly influences people's lives, and requires further attention from  
 114 decision-makers (Zhang and Li, 2019). For this purpose, the main characteristics of water,  
 115 namely biological, physical, chemical, and radiological, are considered as the water quality (Liou

116 et al., 2004). This is the extent of the condition of water regarding the prerequisites of in any  
117 biotic animals and also to any human need. Low quality of surface water that is calculated by  
118 various standards such as the health of ecosystems, the safety of human, and drinking water is a  
119 crucial subject in the developing world, according to which threatens ecosystems and  
120 plants/animals life and human health (Sarkar et al., 2007). Rivers are the most accessible water  
121 resources and has been the primary water supply to human civilizations throughout history  
122 (Mohammadpour et al., 2016). Rivers among various sources of water supply have been utilized  
123 more frequently for human societies' development due to easy access (Ishikawa et al., 2019). The  
124 reason for utilizing rivers instead of other water resources like groundwater and seawater is that  
125 they might have some problems such as land subsidence (Motagh et al., 2017) and pollution  
126 transmission (El-Kowrany et al., 2016), respectively.

127 Many years ago, the Department of Environment (DoE) suggested the reception of WQI to  
128 evaluate and rank the degree of waterways contamination. From that point, the DoE  
129 recommended a methodology called (OP-WQI) which stands for Opinion Poll WQI for  
130 ascertaining the rank the level of water river of nearby waterways. The strategy that utilized for  
131 figuring the WQI in Malaysia includes extensive estimations, changes, devouring time, and  
132 exertion (Hameed et al., 2017). In this manner, suggesting an alternative approach, which is  
133 immediate and faster with high exactness of computing the WQI, is required. The advantage of  
134 water quality index modeling is to provide better management of rivers (Gurjar and Tare, 2019).  
135 For decades, precise prediction models of water quality parameters established by experts like  
136 (Ishikawa et al., 2019).

137 Artificial Neural Networks (ANNs) is one of the outstanding DDMs which have been  
138 successfully applied to address many prediction issues associated with the environment and

139 water resources such as stormwater prediction (Gaafar et al., 2019), wastewater modeling  
140 (Bagheri et al., 2015), heavy metal prediction (Nath et al., 2018), sediment transport modeling  
141 (Moeeni and Bonakdari, 2017), streamflow forecasting (Attar et al., 2020), water level  
142 forecasting (Nayak et al., 2006). Although ANN models increase the capacity of model functions  
143 by training the data sets, it has some disadvantages, including difficulties in assessing the proper  
144 network structure and finding the local optimum, slow convergence rate, and long training time  
145 (Chau, 2006). All prediction and measurement approaches have some errors related to them as  
146 models do not appropriately simulate the whole behavior of the real system (Attar et al., 2018).

147 Data Assimilation (DA) can be a useful technique for the generation of an accurate state  
148 estimation by fusing the data from these sources (Rezaie-Balf et al., 2019b). Predictive model  
149 parameters can be adjusted automatically through DA that is based on mathematic conceptions  
150 (Kashif Gill et al., 2007). The essential of DA is to evaluate errors in the model along with the  
151 observation data and to update model states by combining the model with observations  
152 (Abbaszadeh et al., 2017; Moradkhani et al., 2005).

153 Researchers have proposed various strategies for reducing input/output variables to overcome  
154 non-stationary time series in hydrological parameters (Zhang et al., 2018) These strategies are  
155 known as the pre-processing procedures for improving the original data to noise ratio (Rezaie-  
156 Balf et al., 2019b). Also, the time series variables can be changed into reasonable structures for  
157 further estimation (Dong et al., 2019). Intrinsic Time-scale Decomposition (ITD) is one of the  
158 time-frequency-energy analysis, which is utilized in this investigation to arrange multicomponent  
159 variables into a few Proper Rotation Components (PRCs) and change non-stationary signals into  
160 stationary ones (Martis et al., 2013). In other words, the nonparametric decomposition technique

161 has been influential for the dataset that inherently is nonstationary and nonlinear with minimal  
162 assumptions about data (Yu et al., 2017).

163 This study aims to provide an overview of available DDMs for WQI prediction. Several  
164 predictive models based on soft computing applications have been reviewed here in order to  
165 assess the literature. The core objective of the present research is to develop a new and accurate  
166 hybrid model for predicting WQI using physicochemical parameters in Klang and Langat Rivers,  
167 the two case studies in Malaysia. To the knowledge of the authors, there is no published study  
168 related to the application of the ANN learning machine and the Ensemble Kalman Filter (EnKF).  
169 The main contribution of the study is to address the erroneous noise reduction for both  
170 remarkable improvements in data quality, and prediction accuracy seems to have blurred the  
171 hydrology community on the effectiveness of reduction in nonlinear noise in WQI predicting. So  
172 then, ITD is firstly used in the present study to surmount the non-stationarity issues applying to  
173 decompose the original time series dataset regarding water quality parameters into several sub-  
174 sequences. Different models, therefore, are built for each sub-sequences according to its intrinsic  
175 features. Another purpose of this study is to estimate the robustness of the hybrid ITD-EnKF-  
176 ANN *vs.* other hybrid models such as GD-ANN, EnKF-ANN, and ITD-EnKF-ANN *viz*  
177 analytical calculation of performance with graphical plots and numerical metrics of modeled and  
178 observed WQI data.

## 179 **2. Literature review**

180 WQI is a number that illustrates the sum of water quality parameters as a particular number and  
181 is useful for managers and decision-makers to assess the water quality in any specific site  
182 (Mijares et al., 2019). WQI is introduced in Germany in 1848 (Tasneem Abbasi, Shahid A.,  
183 2012), and Horton proposed the first WQI in 1965 (Robert K, 1965). WQI has ranges by its index

184 numbers, which shows how the water is clean, and it can be classified as excellent quality, good  
 185 quality, poor quality, very poor, and unsuitable for drinking (Khalid et al., 2018). In general,  
 186 water quality indexes are divided into six categories as follows: river WQI, drinking WQI,  
 187 Groundwater WQI, sanitation WQI, irrigation WQI, and WQI in the wetland (Babaei et al.,  
 188 2011). Table 1 provides a list of relevant studies on the application of DDMs in river WQI  
 189 prediction. Also, the participant of physicochemical parameters on the prediction of WQI  
 190 extracting from literature review between 2000 and 2019 are illustrated pH and DO with the  
 191 95.83 and 91.67, respectively, were the most influential parameters researchers considered for  
 192 the studies (Figure 1).

193 **Table 1.** Application of DDM using WQI prediction-literature review from 2000 to 2019.  
 194

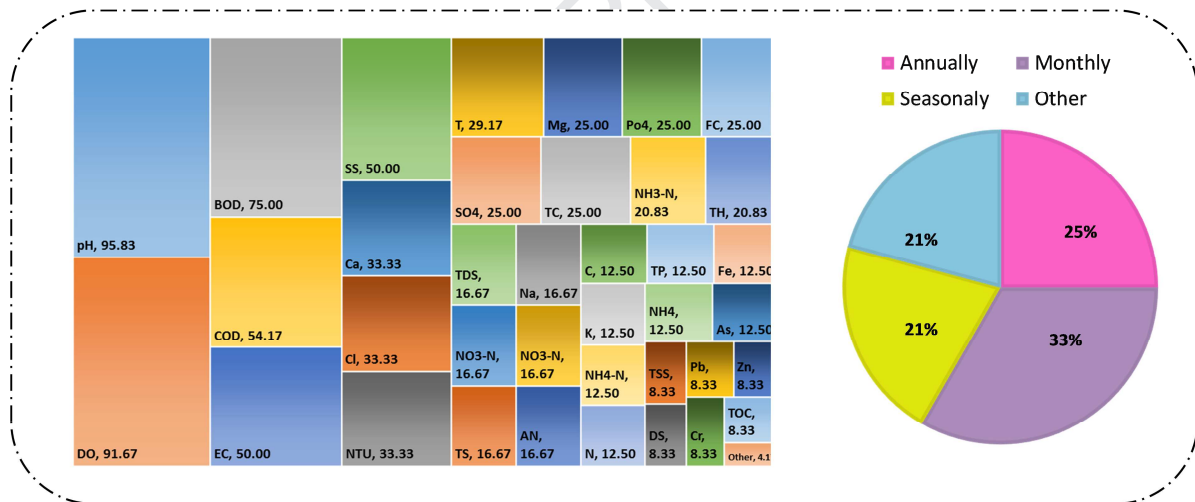
Authors	Year	Model	Time scale	Input Variables	Study Area	Journal
<b>Khuan et. al</b> (Khuan et al., 2002)	2002	ANNs	Annually	DO, BOD, COD, pH, AN, SS	Pahang and Selangor Rivers in Malaysia	Student Conference on Research and Development(IEEE)
<b>Juahir et. al</b> (Juahir et al., 2004)	2004	ANNs	Annually	DO, BOD, SS, AN, COD, pH	Langat River in Malaysia	Journal Kejuruteraan Awam
<b>Ocampo-Duque et. al</b> (Ocampo-Duque et al., 2006)	2006	ANFIS	Monthly	DO, pH, EC, SS, BOD, TOC, TC, FC, Sa, FST, PO4, NO3, NH4, SO4, Cl, F, Atr, BTEX, Ni, Sim, TCB, Cr, HCBd, PAH, As, Pb, Hg	Ebro River in Spain	Environment International
<b>Gazzaz et. al</b> (Gazzaz et al., 2012)	2012	ANN	Monthly	T, EC, DS, pH, NTU, SS, TS, NH3-N, DO, BOD, COD, Na, K, Ca, Mg, NO3-N, Cl, PO4-P, As, Zn, Fe, TC, C	Kinta River in Malaysia	Marine Pollution Bulletin
<b>Amornsaman kul et. al</b> (Amornsaman kul et al., n.d.)	2012	FS, GA	Monthly	pH, DO, TS, FC, BOD, SS, TP, T <sub>air</sub> , T <sub>water</sub>	Thailand	14th international conference on Automatic Control
<b>Sinha et. al</b> (Sinha and	2013	CA, ANNs	Monthly	pH, DO, FC, BOD, TC	The Hooghly River Basin of	Desalination and Water Treatment

(Saha), 2014)						West Bengal in India	
<b>Mohammad pour et. al</b> (Mohammadpour et al., 2016)	2015	SVM	Weekly	T, pH, DO, EC, SS, NO <sub>2</sub> , NO <sub>3</sub> , AN, BOD, COD, PO <sub>3</sub>		Wetland in the Universiti Sains in Malaysia	Environmental Science and Pollution Research
<b>Sahoo et. al</b> (Sahoo et al., 2015)	2015	ANFIS, PCA	Monsoon season	pH, DO, BOD, EC, NO <sub>3</sub> -N, TC, FC, COD, NH <sub>4</sub> -N, TA-CaCO <sub>3</sub> TH-CaCO <sub>3</sub>		Brahmani River in India	Aquatic Procedia
<b>Than et. al</b> (Nguyen Hien Than et al., 2016)	2016	ANNs	Annually	T, Sunshine, Rainfall, Humidity, T <sub>water</sub> , pH, DO, NTU, C, EC		The Dong Nai River in Vietnam	Journal of Environmental Science and Engineering
<b>Babbar et. al</b> (Babbar and Babbar, 2017)	2017	NB, DT, KNN, SVM, ANN, RBC	June 1995–1997	NTU, pH, DO, BOD, TDS, TH, Cl, NO <sub>3</sub> , SO <sub>4</sub> , TC		Yamuna River Basin in India	Environmental Earth Sciences
<b>Ahmad et. al</b> (Ahmad et al., 2017)	2017	MNNs	Weekly	DO, SS, pH, NH <sub>3</sub> -N, T, EC, NTU, DS, TS, NO <sub>3</sub> , Cl, PO <sub>4</sub> , As, Zn, Ca, Fe, K, Mg, Na, OG, E-Coli, C, Cd, Cr, Pb		Perak River Basin in Malaysia	International Journal of River Basin Management
<b>Hameed et. al</b> (Hameed et al., 2017)	2017	ANNs	Monthly	DO, BOD, COD, NH <sub>3</sub> -N, SS, pH		Langat River and Klang River in Peninsular Malaysia	Neural Computing and Applications
<b>Pham et. al</b> (Pham et al., 2017)	2017	HCA, CA, ANOVA	Seasonally	DO, BOD, COD, NH <sub>4</sub> , N, PO <sub>4</sub> , P, TSS, pH		The Upper Part of Dong Nai River Basin in Vietnam	Journal of Water Sustainability
<b>Al-Musawi et. al</b> (Al-Musawi et al., 2017)	2017	ANNs	Annually	pH, PO <sub>4</sub> , NO <sub>3</sub> , Mg, Ca, TH, Na, SO <sub>4</sub> , Cl, TDS, Alk, EC, Fe, NTU		Tigris River of Baghdad in Iraq	Applied Research Journal
<b>Yaseen et. al</b> (Yaseen et al., 2018)	2018	ANFIS	Monthly	DO, TS, NTU, Ca, BOD, COD, T, pH		Selangor River located in Malaysia	Water Resources Management
<b>Wu et. al</b> (Wu et al., 2018)	2018	SMLR	Seasonally	T, pH, DO, EC, NTU, N, P, NH <sub>4</sub> -N, NO <sub>3</sub> , NO <sub>3</sub> -N, Ca, Mg, Cl, SO <sub>4</sub>		In Lake Taihu Basin in China	Science of the Total Environment
<b>Wang et. al</b> (Wang, 2018)	2018	SVR, PSO-SVR	October 2016	COD, DO, pH, NTU, EC, TP, TN, NH <sub>4</sub> -N, NO <sub>2</sub> -N, NO <sub>3</sub> -N, Ca, Mg, Cl, SO <sub>4</sub> , T <sub>water</sub>		Ebinur Lake in China	Nature, Scientific Reports
<b>Tiwari et. al</b> (Tiwari et al., 2018)	2018	ANFIS	Annually	DO, BOD, TDS, SS, NH <sub>3</sub> -N, N, TP, FC		River Satluj in India	Advances in Civil Engineering

<b>Yilma et. al</b> (Yilma et al., 2018)	2018	ANNs	Seasonally	TSS, N-NO <sub>3</sub> , N-NO <sub>2</sub> , TN, TA, TOC, COD, BOD, DO, T, EC, pH	Little Akaki River in Addis Ababa, Ethiopia	Modeling Earth Systems and Environment
<b>Leong et. al</b> (Leong et al., 2019)	2019	SVM, LS-SVM	Annually	DO, BOD, COD, SS, pH, AN	Perak State in Malaysia	International Journal of River Basin Management
<b>Kumar et. al</b> (Kumar et al., 2019)	2019	MSA	March 2012	pH, T, DO, BOD, COD, TN, NH <sub>4</sub> , TC, FC	Yamuna River in India	International Journal of River Basin Management
<b>Kadam et. al</b> (Kadam et al., 2019)	2019	ANNs, MLR	Pre and post-monsoon seasons	pH, EC, TDS, TH, Ca, Mg, Na, K, Cl, HCO <sub>3</sub> , SO <sub>4</sub> , NO <sub>3</sub> , PO <sub>4</sub>	Shivganga River Basin in India	Modeling Earth Systems and Environment
<b>Kükrer et. al</b> (Kükrer and Mutlu, 2019)	2019	MSA	Monthly	pH, T, EC, SS, BOD, TH, TA, Ca, N, NH <sub>3</sub> , Cu, DO	Saraydüzü Dam Lake in Turkey	Environmental Monitoring and Assessment
<b>Ho et. al</b> (Ho et al., 2019a)	2019	DT	Monthly	NH <sub>3</sub> -N, BOD, COD, DO, pH, SS	Klang River in Malaysia	Journal of Hydrology

195

196



197

198 **Figure 1.** The participation of physicochemical parameters on the prediction of WQI extracted  
 199 from the literature review between 2000 and 2019.

200

201 Chang et al. (Chang et al., 2001) considered three fuzzy synthetic evaluation approaches to  
 202 model Taiwan river water quality at the Tseng-Wen river system. The results demonstrate that a  
 203 fuzzy synthetic evaluation method could be useful for daily total maximum load prediction.

204 Khuan et al. (Khuan et al., 2002) predicted WQI for three years for rivers in Pahang and  
205 Selangor in Malaysia by using three algorithms of the ANN, including backpropagation, modular  
206 neural network, and radial basis function. Results showed that the RBFN algorithm had higher  
207 accuracy than the two other models. Khan et al. (Khan et al., 2003) assumed two different  
208 standard indexes namely British Columbia water quality index (BWQI) and Canadian water  
209 quality index (CWQI) to estimate WQI in specific watersheds of the region of Atlantic: the  
210 Point Wolfe River, the Mersey River, and the Dunk River of Canada. The results of this study  
211 assess each standard indexes.

212 Juahir et al. (Juahir et al., 2004) tested ANN, and multiple linear regression (MLR) approaches  
213 for modeling WQI in the site of the Langat River Basin, Malaysia. They showed that  
214 Biochemical Oxygen Demand (BOD), Chemical Oxygen Demand (COD), Dissolved Oxygen  
215 (DO), Ammoniacal-Nitrate (AN), Suspended Solids (SS), and pH were contributed to the  
216 estimation of WQI. The results indicate that with omitting two parameters, namely COD and pH  
217 as independent variables, the accuracy of the ANN model could be better. Ocampo-Duque et al.  
218 (Ocampo-Duque et al., 2006) stated fuzzy inference systems as a model for estimation WQI in  
219 Ebro River (Spain). The outcomes of this study have led to proper linking between fuzzy  
220 inference systems and parameter weighting approaches. Hore et al. (Hore et al., 2008) utilized  
221 the artificial neural network to estimate WQI by accessing waste and polluted water from  
222 industrial waste. Two algorithms, namely multilayer-perceptron (MLP) with a back-propagation,  
223 were used in this study. As a result, they found that ANN was a convincing method in WQI  
224 prediction. Lermontov et al. (Lermontov et al., 2009) used a fuzzy water quality index in order to  
225 predict WQI in Ribeira do Iguape River watershed in Brazil. They introduced a new Index as the

226 fuzzy water quality index (FWQI), and the results of this study showed a good correlation with  
227 the traditional calculated index.

228 Roveda et al. (Roveda et al., 2010) evaluated fuzzy logic in a case of Sorocaba River to model  
229 WQI, and they tried to compare the estimated WQI with CETESB WQI (Companhia de  
230 Tecnologia de Saneamento Ambiental, in Brazil). They found that it is better to use this  
231 estimated method instead of CETESB. Mahapatra et al. (Mahapatra et al., 2011) evaluated the  
232 Fuzzy Inference System for estimating WQI in India by utilizing two methods of Sugeno,  
233 Takagi, Mamdani, and Kang (TSK) models. The results of this study were compared with three  
234 international WQI criteria, and it was found that the cascaded fuzzy system has precious results.  
235 Gazzaz et al. (Gazzaz et al., 2012) presented ANN to model WQI for the Kinta River in Malaysia  
236 with three categorical variables, including watercolor, water level, and weather, and 32  
237 parameters. The algorithm of ANN called quick propagation training algorithm was defined as  
238 the best algorithm to model WQI. Sinha & Saha (Sinha and (Saha), 2014) evaluated the  
239 reliability of artificial neural network and cluster analysis modeling in the case of the Hooghly  
240 River basin in India for WQI estimation. They tried to compare the results of these methods of  
241 DELPHI and CCME, and they found that the DELPHI method has the superior ability in WQI  
242 estimation rather than the CCME method.

243 Hameed et al. (Hameed et al., 2017) investigated artificial intelligence techniques with two  
244 different algorithms, namely BPNN and RBFNN, to model WQI in the tropical region in  
245 Malaysia. They have used six water quality parameters, including DO, NH<sub>3</sub>-N, COD, SS, BOD,  
246 and pH. Results demonstrated that the RBFNN algorithm performed better than BPNN, which  
247 has higher precision. Babbar & Babbar (Babbar and Babbar, 2017) evaluated water quality  
248 index applying techniques of data mining as flows: artificial neural networks, naive Bayes,

249 decision trees, k-nearest neighbors, and support vector machines. Parameters that are used to  
250 their study were pH, chlorides, DO, BOD, total coliforms total dissolved solids (TDS), sulfates,  
251 hardness, nitrates, and turbidity. They detected that the decision tree and support vector machine  
252 classifiers are the best models among the other DDMs.

253 Kisi and Yaseen (2019) analyzed alternative hybrid models based on grid partition and  
254 subtractive clustering models and adaptive neuro-fuzzy inference system (ANFIS) integrated  
255 with fuzzy c-means data clustering, in order to model WQI in Selangor river basin in Selangor  
256 by utilizing WQI parameters namely temperature, DO, BOD, turbidity (TU), total suspended  
257 solids (TSS), calcium (Ca), COD, and pH. The results demonstrate that in the case of accuracy,  
258 ANFIS-SC and ANFISFCM have better results in comparison to the ANFIS-GP model. Ho et al.  
259 (2019a) employed decision tree machine learning techniques accompanied by different scenarios  
260 (different inputs) for Klang river in Malaysia with six water quality parameters such as NH<sub>3</sub>-N,  
261 DO, BOD, COD, SS, and pH in order to predict WQI. The results indicate that the number of  
262 water quality parameters can be diminished as NH<sub>3</sub>-N, SS, and pH because of a less significant  
263 outcome on WQI prediction in a monitoring process. Leong et al. (2019) outlined the use of a  
264 support vector machine (SVM) and least-square SVM in WQI modeling. The DoE approach  
265 (Malaysia formula to calculate WQI) was used and considered six variables, including DO, SS,  
266 BOD, COD, AN, and pH value. As a result, it is found that the LS-SVM model performs better  
267 than the SVM model.

268 By reviewing relevant literature, it is observed that most of them used ANN, ANFIS, and SVM  
269 to predict WQI without considering uncertainty in models' parameters. That is modest changes  
270 to these parameters can significantly alter the model output, making their uncertainty a serious  
271 source for predict errors. Therefore, in this study, the feasibility of estimating parameters

272 simultaneously with the dynamical state is investigated using EnKF by means of state space  
273 augmentation. Monitoring and reducing the noise, non-stationary, non-linearity, and complexity  
274 of the time series data can be another gap that was not taken into account in previous studies.  
275 Prior to using input time series data in the model development process, the frequency  
276 components should be resolved to enhance the accuracy of the model. Hence, ITD is a  
277 decomposition tool available to address such issues to precisely reconstruct the original time  
278 series data and give an appropriate spectral separation of sub-series.

### 279 **3. Case studies and available data**

280 Adequate water resources are essential for overall economic prosperity in a developing country  
281 such as Malaysia (Najah Ahmed et al., 2019). However, some areas in Malaysia are currently  
282 experiencing water shortages, even though large amounts of water reserves are available (Naubi  
283 et al., 2016). This growing need for water is due to the growth in population, urbanization,  
284 industrialization, and irrigated agriculture have dramatically increased the demand for alternative  
285 water supplies (Ho et al., 2019b). During the monsoon season, most flood-prone areas  
286 experience flooding or flash floods that cause loss of lives, damage to property, and destruction  
287 of crops. According to (Ahmed et al., 2019), due to changing weather patterns, this situation will  
288 only get worse, and Malaysia has to improve its pre-disaster management systems in order to  
289 avoid further damage and other adverse effects caused by floods in the future.

290 Before focusing on the core of the study (developing water quality prediction model), it is  
291 necessary to provide an overview of the climate condition in the selected study area. This is due  
292 to the fact that the climate condition could be essential for the model generalization ability for  
293 future research. The climate condition for both river basins is the same as both are located in the  
294 tropical zone in Malaysia. In general, the Malaysian's climate is affected by several regional and

295 global phenomena such as El Nino, Indian Ocean Dipole (IOD), and monsoons (Suhaila et al.,  
296 2010). These phenomena played a vital role in the hydrological formation of the whole country  
297 and, more specifically, the extreme events of the rainfall along with the whole year. The annual  
298 rainfall is almost 2000 mm, and the highest recorded rainfall was 330 mm that has been  
299 experienced in November. On the other hand, the lowest record has occurred in June with almost  
300 100 mm (Tangang et al., 2012).

301 Seasonally, two major monsoon regimes influenced the climate in Malaysia, namely; Northeast  
302 (NE) and Southwest (SW) monsoon patterns. The SW monsoon season that is dominated by the  
303 low-level south-westerly winds begins in May and lasts through August. On the other hand, the  
304 NE monsoon season that is controlled by the northeast wind commences in November and ends  
305 in February of the following year (Tan et al., 2019). In terms of the temperature pattern in both  
306 study areas, the maximum temperature that has been recorded during the last 40 years ranged  
307 between 32°C and 35°C, while the minimum temperature was ranged between 21°C and 25°C.  
308 From these records, it could be noticed that the narrow changes in the range of temperature,  
309 whether the maximum or the minimum ones, showed that the temperature might not play a  
310 significant influence on the water quality pattern (Palizdan et al., 2015).

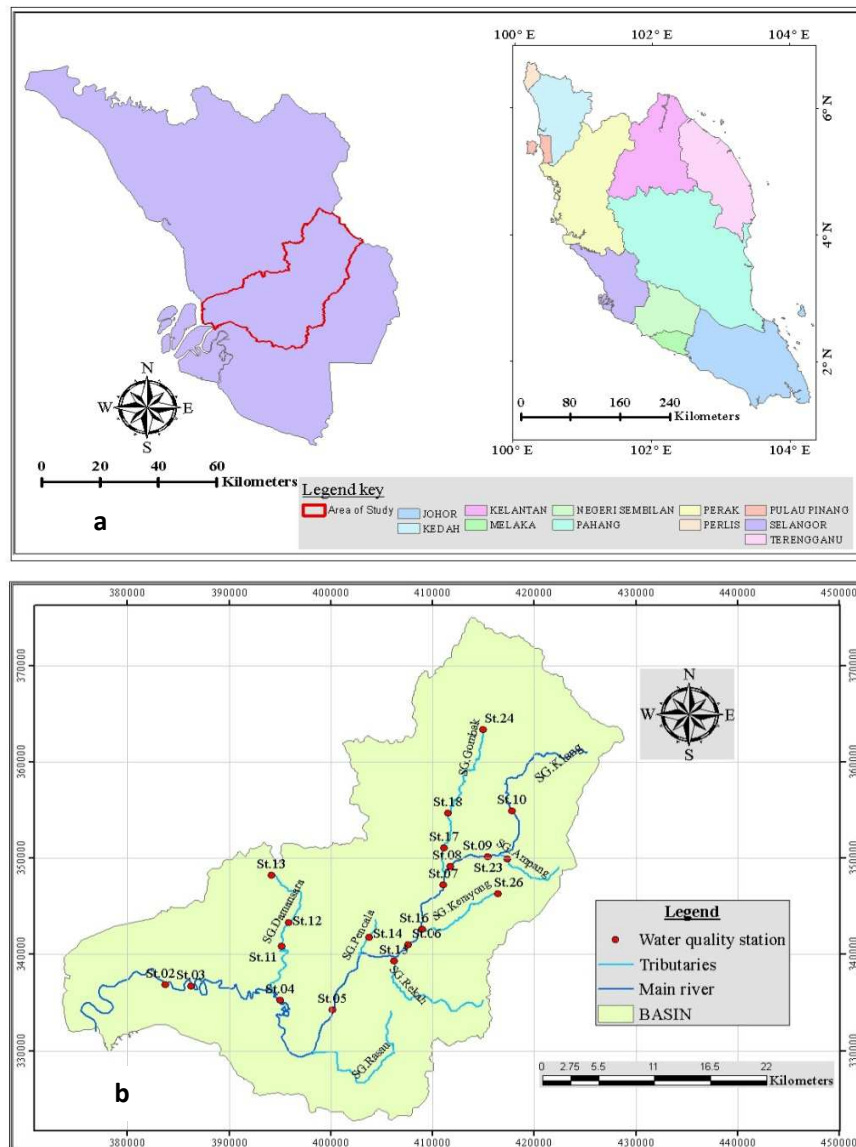
311 Recent research showed that there might not a significant change in the climate condition in  
312 Malaysia in the short and medium terms. However, it is expected that there might be a gradual  
313 change in the long-term trend changes in the rainfall and temperature patterns. In this context, in  
314 the long-term, such significant changes in the seasonal or annual rainfall and the maximum and  
315 minimum temperature could drive to changes in the water quality patterns. This is due to the fact  
316 that such changes could influence on the flood and drought frequency and hence the availabilities

317 of the freshwater. Also, it has been observed that the monsoon phenomenon is the most powerful  
318 system on the climate condition in Malaysia (Soo et al., 2019).

319 In the present study, in order to examine the proposed models' performances, two different case  
320 studies were chosen, namely the Klang River and the Langat River. In the following subsections,  
321 details about the water resources and water quality for both rivers would be explained.

### 322 **3.1. The Klang River**

323 The Klang River stretches approximately 120 km through the two most populated areas in  
324 Malaysia; the State of Selangor and the Wilayah Kuala Lumpur. The river flows from the Ulu  
325 Gombak Forest Reserve to Port Klang and on into the Straits of Malacca, one of the busiest  
326 shipping lanes in the world. The Klang River basin is the country's most inhabited region, with  
327 more than four million residents. This area contains several main cities of the Selangor State and  
328 Wilayah Kuala Lumpur, such as Klang, Shah Alam, Puchong, and Petaling Jaya. The biggest  
329 seaport in Malaysia, Port Klang, is also situated on the estuary of the Klang River (Juahir et al.,  
330 2004). The Klang River's watershed covers approximately 1,288 km<sup>2</sup> of the storage basin. This  
331 region has witnessed the country's strongest economic growth, and 35 % of the area has been  
332 built up for residential, commercial, industrial and institutional purposes. This region is also  
333 considered to be polluted as the extensive developments along the river basin due to the illegal  
334 discharge of unprocessed wastewater, as well as treatment plant and animal farming waste,  
335 which has deteriorated the water quality of the river. Figure 2 illustrates the location of the river  
336 in Malaysia and the location of the water quality monitoring stations.



337

338

339

340

341

**Figure 2.** a) Location of Klang River Catchment and b) water quality monitoring stations

342 The Klang River serves as the primary water supply source for Selangor and Kuala Lumpur,  
 343 providing nearly 1,128.4 million liters per day (DOE, 2007).

344 The data selected for the present study were monthly water quality parameter assessment data,  
 345 summarized as WQI. The six physicochemical water quality parameters used to calculate the

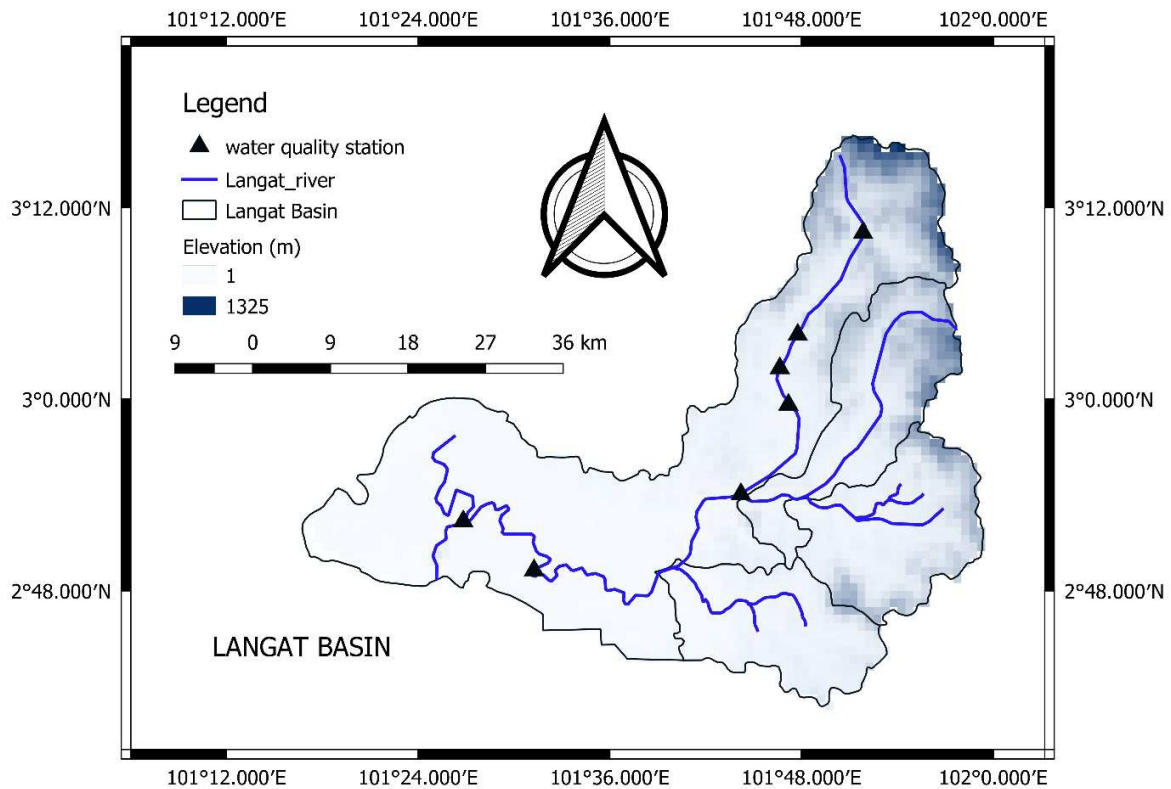
346 WQI was biochemical oxygen demand (BOD), chemical oxygen demand (COD), dissolved

347 oxygen (DO), suspended solids (SS), pH and ammoniacal nitrogen (NH<sub>3</sub>-N). The data were  
348 collected from monitoring stations situated on the Klang River (Yahya et al., 2019). A total of  
349 305 data samples were accumulated for the duration between January 2005 and August 2016 for  
350 this study (Palizdan et al., 2015).

### 351 **3.2. The Langat River**

352 One of Malaysia's most important rivers, the Langat River, is regarded as the primary source for  
353 agriculture, consumption, farming, and fishing in the state of Selangor (see Figure 3). The Langat  
354 River runs west across the Langat Basin to Kuala Langat from the highest point of the 1,493 m in  
355 the Titiwangsa Range. It then flows into the Straits of Malacca. It is 78 km long discharges an  
356 area of 2,350 km<sup>2</sup>. The Langat River is mainly characterized by water bodies (e.g., natural lakes),  
357 forests, agriculture, and urban residential and commercial areas. The types of forests within the  
358 catchment area are mangrove, dipterocarp, and swamp. The dominant land-use within the  
359 catchment area is for agricultural purposes.

360



361

362

**Figure 3.** Location of the Langat River Catchment

363 Land-use practices along the banks of the river have led to the degradation of the water quality of  
 364 the river (Najah et al., 2011). Research by Yahya et al. (Yahya et al., 2019) determined that the  
 365 main factors contributing to differences in the quality of the Langat streamflow were the  
 366 development of the wastewater treatment plants and the industrial waste (chemical effluents), as  
 367 well as runoff from domestic and commercial areas.

### 368 3.3. Available data

369 In 1978 DoE established baselines to detect the water quality changes in river water quality and  
 370 has since been extended to identifying pollution sources as well. Water samples are collected at  
 371 regular intervals from Water samples that have been collected from designated stations for in--  
 372 situ and laboratory analysis to determine physicochemical and biological characteristics. Water  
 373 quality monitoring activities were privatized to ASMA (Alam Sekitar Malaysia Sdn Bhd) on 1st

374 January 1995, both manual & automatic monitoring. In 2005, 1064 manual stations in 146 river  
375 basins were monitored (Thorough review of river basins & monitoring stations in 2004).  
376 Parameter for in-situ measurement are DO (%), DO (mg/l), Turbidity (NTU), Conductivity  
377 (uS/cm), Salinity (ppt), pH, Temperature (T). While the parameter for lab analysis are: BOD,  
378 COD, SS, NH<sub>3</sub>-N, pH, DS, TS, NO<sub>3</sub>-N, Cl, PO<sub>4</sub>-P, O&G, MBAS, E.coli, Coliform, As, Hg, Cd,  
379 Cr, Pb, Zn, Ca, Fe, K, Mg, Na [ 24 chemical and biological parameters ]. There are three types of  
380 monitoring stations that have been used by DoE to identify the water quality parameters. The  
381 first type is the baselines stations that allocated in the far upstream position of the river, which is  
382 only considered for reference and not for detecting the real water quality status of the river as the  
383 river did not affect by the water users. The second type is ambient stations used for monitoring  
384 the water quality, and their records are used to configure the change in the water quality  
385 parameters. These stations are located along with the whole river to detect the point and non-  
386 point sources of pollution. While the third type of the station is the impact station. This type is  
387 used for enforcement purposes and not for the calculation of the real water quality status of the  
388 river.

389 The data is available in, owned by DoE, and could be shared for research purposes. The data  
390 have been collected from DoE, who operates these monitoring stations for both Klang and  
391 Langat rivers, which is institute in charge to monitor the water quality for all rivers in Malaysia.  
392 In the present study, DoE (DOE, 2007), Malaysia provided the water quality records for the  
393 Langat River. The data of the water quality were recorded irregularly with respect to particular  
394 time intervals; therefore, quarterly data were instead used to expedite the study. Consequently,  
395 the present study utilized time-series water quality data (ranging from September 2002 to August  
396 2016) at several monitoring stations for the required parameters. Because this research utilized

397 three-monthly record data, the data reflecting the first quarter were drawn from that quarter's last  
398 month, i.e., from March. Likewise, June data reflected the results for the second quarter.  
399 On the other hand, for the last month of a specific quarter, if there were no data available, data  
400 were then taken from any of the other months within this quarter. For instance, the data  
401 representing Quarter 1 were obtained from either January or February. Similarly, data from April  
402 or May were used to reflect the data for Quarter 2. In order to ensure the development of a  
403 reliable model, it is required to utilize regular data monitoring. In this context, the proposed  
404 model in this study has been developed based on the steady acquired water quality data.  
405 The main reason for the selection of these periods (2005 to 2016 for Klang River and 2012 to  
406 2016 for Langat River) is that the monitoring program for the water quality parameters during  
407 these periods was more reliable. In fact, it is essential to develop the model relying on reliable  
408 data in order to achieve a successful model structure. In this context, it was decided to utilize the  
409 available reliable data during these periods to develop the proposed model.

## 410 **4. Methods**

411 This section is categorized into six parts including determination of WQI as a national index, an  
412 artificial neural network with its formulation, ensemble Kalman filter as a data assimilation  
413 technique, intrinsic time-scale decomposition method, description of ITD-based WQI prediction  
414 models and in the last part, the performance of the models was assessed.

### 415 **4.1. Determination of WQI**

416 As defined by the US Foundation of National Sanitation, WQI varies from 0 to 100, where high  
417 water quality results in the high value of WQI, and lower values of WQI represent the low  
418 quality of water (Said et al., 2004). In 1974, the DoE Malaysia endorsed an index to evaluate the  
419 surface water quality in Malaysia. Thoroughly, six parameters were chosen as chief water quality

420 variables to develop and calculate WQI, such as DO, COD, SS, NH<sub>3</sub>-N, BOD, and pH for  
421 surface water (Khan et al., 2003). These variables should be transformed into a non-dimensional  
422 parameter that the relationship for each parameter can be seen from (Gazzaz et al., 2012), which  
423 has the best-fit relations of parameters. WQI can be obtained considering the following equation  
424 (Khuan et al., 2002):

425

$$426 \quad WQI = 0.22SI_{DO} + 0.19SI_{BOD} + 0.16SI_{COD} + 0.15SI_{NH_3-N} + 0.16SI_{SS} + 0.12SI_{pH} \quad (1)$$

427

#### 428 **4.2. Artificial Neural Networks**

429 Artificial Neural Networks (ANNs) is one of the most fruitful and brain neurological based  
430 black-box methods in modeling environmental issues, specifically in water quality modeling  
431 (Gazzaz et al., 2015). The central aspect of ANNs is the estimation of nonlinear models with  
432 input data and resulted in the output data while using specific functions and algorithms by  
433 learning from an example (Maier et al., 2010). This model typically depends on the architecture  
434 of networks, the hidden layers, and nodes. ANN models can be categorized into varied categories  
435 according to which gradient descent model (GD) is one of the learning approaches. One of the  
436 most critical mathematical optimization methods in GD is backpropagation that is applied for  
437 learning the connection weights of algorithms in ANN models. The gradient descent model  
438 usually attempts to minimize the root-mean-square error (RMSE) by utilizing the  
439 backpropagation algorithm. As aforementioned, the ANN model influenced by the architecture  
440 of neural networks. Multi-layer perceptron is one of the most usual and popular feedforward  
441 types of ANNs architecture and functions for modeling in nonlinear occurrences (Rezaeian-  
442 Zadeh et al., 2012). Single neurons titled perceptron is the basis of this network. This  
443 architecture involves three layers, including input, hidden, and output layers. The hidden and

444 output layers contain a specific amount of neurons, but the input layer will vary by the data  
 445 dimensions. The weights ( $w$ ) connecting layers are defined by training algorithms that utilize the  
 446 BP algorithm. Bearing above in mind, algorithms use the Levenberg-Marquardt algorithm for  
 447 their function approximations. Further information about this typical neural network architecture  
 448 could be found (Taud and Mas, 2018).

### 449 **4.3. Ensemble Kalman filter**

450 Data assimilation is the technique which is dealt with errors in model parameters, uncertainties in  
 451 the models, boundary conditions errors and etc. One of the prominent data assimilation structures  
 452 is the Kalman filter, which was proposed by (Kalman, 1960) for linear systems. Ensemble  
 453 Kalman filter (EnKF) was first introduced by (Evensen, 1994) as an extended Kalman filter. The  
 454 application of EnKF is based on an ensemble of simulations, which can represent the distribution  
 455 of the system (Johns and Mandel, 2008). Unlike the Kalman filter, EnKF can suit for nonlinear  
 456 models (e.g., hydrological models). The background of this model is based on the approach of  
 457 Monte Carlo, in which probability density is the representation of the state (Clark et al., 2008). In  
 458 the state of ensemble data assimilation generation, two errors should be worth considering,  
 459 namely internal and external error. Consider the system of a stochastic, nonlinear, general model,  
 460  $M$  and the observations (Kalman, 1960),

461

$$462 \quad x^f(t_k) = M[x^f(t_{k-1}), U(t_{k-1})] + \omega(t_{k-1}) \quad (2)$$

463

$$464 \quad y^0(t_k) = H(t_k)x^f(t_k) + \vartheta(t_k) \quad (3)$$

465

466 where the forecast represented by  $x^f(t_k) \in R^n$  of the system state at the time  $t_k$ , the system  
 467 forcing  $U(t_{k-1})$ , and the one-time step of the model showed with  $M$ . It is compulsory to  
 468 combine the measurement taken from the observation and modeled by Equation (2), to gain an  
 469 optimum approximation. By using the information given by the system model Equation (3). The  
 470 forecast state at the time  $t_k$ , denoted by  $x^f(t_k)$ , is the forecast from observation time  $t_{k-1}$  to  
 471 observation time  $t_k$  by the following Equation,

$$472 \quad x^f(t_k) = M[x^a(t_{k-1}), U(t_{k-1})] \quad (4)$$

473

474 where  $x^a(t_{k-1})$  is the modeled system state. In  $t_k$ , an observation  $y^o(t_k)$  is existed, and the  
 475 investigation step restructures the model,

$$476 \quad x^a(t_k) = x^f(t_k) + K[y^o(t_k) - H(t_k)x^f(t_k)] \quad (5)$$

477 where,

$$478 \quad K(t_k) = P^f(t_k)H(t_k)^T[H(t_k)P^f(t_k)H(t_k)^T + R]^{-1} \quad (6)$$

479 are the minimum variance gain and the covariance matrix of modeled error represented by  
 480  $P^f(t_k)$ . The covariance in the EnKF algorithm can be estimated by randomly generated a finite  
 481 number of system states. In order to estimate  $x_0$  as an initial value, an ensemble  $\varepsilon_i^f, i = 1, \dots, N$   
 482 of the uncertainty is stated for randomly generated states. Original model operator causes the  
 483 ensemble members to are transmitted from a one-time step to another (Karunasingha and Liong,  
 484 2018),

$$485 \quad \varepsilon_i^f(t_k) = M[\varepsilon_i^a(t_{k-1}), U(t_{k-1})] + \omega_i(t_{k-1}) \quad (7)$$

486

487 Where,  $\omega_i(t_k)$  apprehensions of the noise process. This noise is a supplementary component for  
 488 uncertain parts of the model to estimate the covariance between observation and modeled WQI

489 indices. More information and detailed mathematical background of the ensemble Kalman filter  
 490 could be found at (Maxwell et al., 2018).

491

#### 492 **4.4. Intrinsic Time-scale Decomposition**

493 Intrinsic Time-scale Decomposition (ITD) is a time-frequency representation presented by (Frei  
 494 and Osorio, 2007) for complex and non-stationary time series hydrologic datasets. Proper  
 495 Rotation Components (PRCs) are components in which the datasets are divided into them.

496 ITD process procedures could be divided into some steps. This method has an operator  $L$ , which  
 497 extracts the baseline signal from the input signal  $x(t)$  that resulted in an accurate rotation and  
 498 lower frequency in residuals (Frei and Osorio, 2007). In which  $Lx(t) = Lx(t)$  is the mean of the  
 499 signal, written as  $L(t)$ . The proper rotation components (PRCs) are defined as  $Hx(t) = (1 -$   
 500  $L) x(t)$  which is written as  $H(t)$ . Then decomposed the input signal  $x(t)$  as:

$$501 \quad x(t) = Hx(t) + L(t) = (1 - L) x(t) \quad (8)$$

502 ITD algorithm follows four steps, including:

503 Step 1; Finding the corresponding occurrence time  $\tau_k$  and the extreme points of input signal  $x(t)$ ,  
 504 where  $k = 0, 1, 2, \dots$ . Considering  $\tau_0 = 0$  as the first signal.

505 Step 2; Considering the input signal  $x(t)$  on the interval  $[0, \tau_k + 2]$  and  $L(t)$  and  $H(t)$  as operators  
 506 over the time interval  $[0, \tau_k]$  in which the baseline-extracting operator  $L$  is defined as linear  
 507 function on the interval  $[\tau_k, \tau_k + 1]$ . The baseline extraction operator is designed as:

$$508 \quad Lx(t) = L(t) = L_k + \left( \frac{L_{k+1} - L_k}{x_{k+1} - x_k} \right) (x(t) - x_k), t \in (\tau_k, \tau_{k+1}), \quad (9)$$

509 and

$$510 \quad L_{k+1} = \alpha \left[ x_k + \frac{(\tau_{k+1} - \tau_k)}{\tau_{k+2} - \tau_k} (x_{k+1} - x_k) \right] + (1 - \alpha)x_{k+1} \quad (10)$$

511 Where  $0 < \alpha < 1$  is a constant value and taken as fixed value of ( $\alpha = 1/2$ ). Linearly contraction of  
 512 original signal built in order to make monotonic  $x(t)$  between the extrema points, which is  
 513 necessary for PRCs.

514 Step3; The following operator, were defined for extracting PRCs:

$$515 \quad H(t) = Hx(t) = x(t) - L(t) = x(t) - L(t) \quad (11)$$

516 The main purpose of ITD is to integrate higher signals into several PRCs. As shown in Equation  
 517 11, by subtracting the baseline from the input signal, PRCs can be attained. The advantages of  
 518 ITD can be summarized in three concepts; low computational time, avoiding transient  
 519 smoothing, solving the smearing in time-scale space, and constant sifting (this process is applied  
 520 to data iteratively in order to generate optimum PRCs).

521 Step4; This process of equations 9 and 10 iteratively repeated until the baseline  $L(t)$  converts to a  
 522 monotonic function in which the single signal can be divided into PRCs.

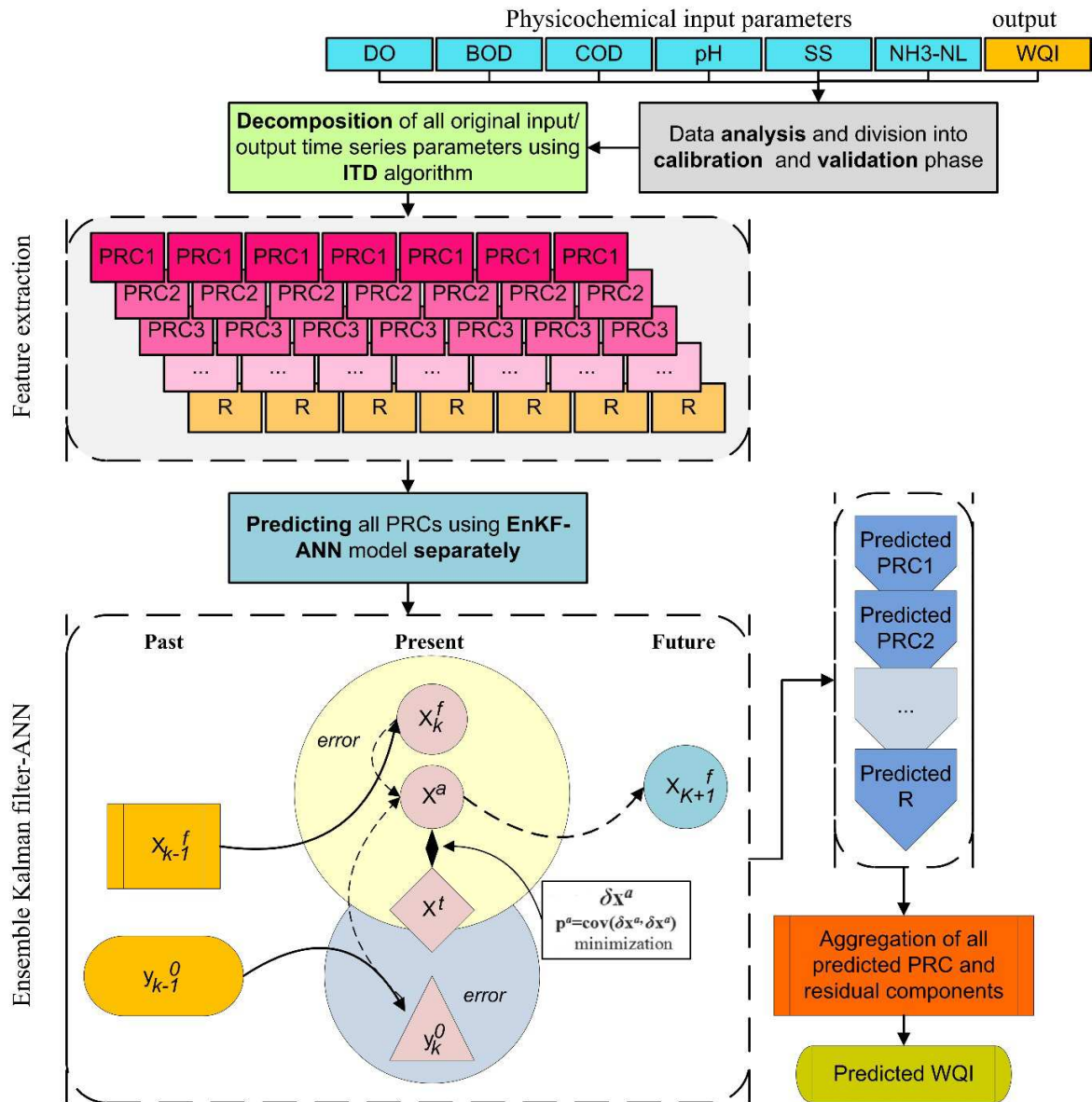
$$523 \quad x(t) = \sum_{i=1}^p H^i(t) + L^p(t), \quad (12)$$

524 where  $p$  is the number of achieved PRCs.

525

#### 526 **4.5. Description of ITD-based WQI prediction models**

527 The primary purpose of ITD-based DDMs is to predict the WQI using physicochemical  
 528 parameters at two different rivers in Malaysia. The schematics of the ITD-EnKF-ANN, which is  
 529 considered to predict WQI at two stations, is shown in Figure 4. Before starting three main steps  
 530 of decomposition-based models, a total of physicochemical measurements and WQI over a  
 531 monthly time-scale should be divided into two separate parts, calibration (a total of 75 % of data)  
 532 and validation phases (the remaining 25 %), the ideal model is selected independent of the  
 533 calibration stage.



534

535 **Figure 4.** The schematic structure of the proposed hybrid (ITD-EnKF-ANN) model integrating  
 536 intrinsic time-scale decomposition (ITD) pre-processing approach with an artificial neural  
 537 network (ANN) model based on the ensemble Kalman filter (EnKF).

538

539 The number of the model parameters and the randomness of data is two factors which based on  
 540 them, the number of data points could be calculated (Fijani et al., 2019). In this research, little

541 random variations of the data revealed that a reasonable model with a sufficient number of  
542 available observations could be estimated.

543 By considering (Rezaie-Balf et al., 2019a) study, three essential steps to enhance the  
544 performance of proposed models can be followed by:

545 Step 1: ITD procedure is used to break down the input and output datasets into several PRC and  
546 one residual components.

547 Step 2: The GP/EnKF-ANN models are proven as WQI estimation tools to calculate the  
548 decomposed PRC and to calculate each component using the same sub-series (PRC1) and  
549 the residual component of input variables respectively.

550 Step 3: The forecasted values of all extracted PRC and residue components using both  
551 GP/EnKF-ANN models are combined to generate the WQI.

552 To summarize, the ITD-based DDMs (i.e., ITD-GP-ANN and ITD-EnKF-ANN) emphasize the  
553 “*decomposition and ensemble*” idea. The decomposition is to facilitate the predicting procedure.  
554 Whereas, the ensemble is to formulate a consensus estimating on the original datasets. In this  
555 work, for verifying and making the pattern of the extracted PRCs and residual components to  
556 reflect the estimation technique and improve the prediction process, two rivers in Malaysia (e.g.,  
557 Klang and Langat) are selected.

558 It should be mentioned that in step 2, how the ANN hybridized with a Kalman filter to predict  
559 each decomposed PRC and residuals components. In the combined approach, the state vectors  
560 are provided to the EnKF technique in which the output of the ANN will be considered as state  
561 vectors. The output of the ANN will correct by the EnKF to determine the best estimate of the  
562 analyzed state or system using the observation data. These states will have resumed all the inputs  
563 of the ANN model for the following time step. The inputs of this network have some differences

564 within them, which are related to feedback form loop or force. For more details, one of the  
 565 hybridizations of EnKF and ANN the readers can be addressed to (Sharma and Lie, 2012).

#### 566 **4.6. Model's performance metrics**

567 In this study, the newly implemented hybrid ITD-EnKF-ANN vs. ITD-GD-ANN, and standalone  
 568 EnKF-ANN and GD-ANN models were evaluated by several standard statistical criteria during  
 569 WQI prediction. Besides common criteria such as RMSE, Nash-Sutcliffe Efficiency (NSE), and  
 570 Mean Absolute Error (MAE), to assess the fidelity of hybrid proposed models below indices  
 571 were applied.

572 1. Kolmogorov-Smirnov distance (K-S distance): It measures the maximum distance D between  
 573 two consecutive cumulative distribution functions (CDF) (Justel et al., 1997).

$$574 \quad D_i = \max|F_{i-1}(x) - F_i(x)| \quad (13)$$

575 2. The ratio of RMSE to Standard Deviation (RSD): RSD metric, was first introduced by (Singh  
 576 et al., 2005), which is a model evaluation metric to assess the variations between the predicted  
 577 and observed WQI data. This metric is calculated based on two error metrics, namely, standard  
 578 deviation (STDEV) and RMSE of the observed WQI data points. The lower value of RSD shows  
 579 the higher performance of the model.

$$RSD = \frac{RMSE}{STDEV_{obs}} = \frac{\left[ \sqrt{\sum_{i=1}^N (WQI_{obs} - WQI_{pre})^2} \right]}{\left[ \sqrt{\sum_{i=1}^N (WQI_{obs} - \overline{WQI_{obs}})^2} \right]} \quad (14)$$

580 3. Uncertainty at 95 % (U95): U95 is considered as a 95 % uncertainty confidence of the model.

$$U_{95} = 1.96\sqrt{(STDEV^2 + RMSE^2)} \quad (15)$$

581 4. Reliability of model (%): This statistical metric indicates the satisfactory state of the model's  
 582 prediction rate by the probability.

$$Reliability = \frac{\sum_{i=1}^N K_i}{N} \times 100 \% \quad (16)$$

$$K_i = \begin{cases} 1, & \text{if } (RAE_i \leq \delta) \\ 0, & \text{else} \end{cases} \quad (17)$$

$$RAE_i = \frac{|WQI_{pre}(i) - WQI_{obs}(i)|}{WQI_{obs}(i)} \times 100 \%, \quad RAE_i \geq 0 \quad (18)$$

583 5. The resilience of model (%): This indicator defines how rapidly the model forecast is likely to  
 584 recover once an unqualified prediction has followed (Zhou et al., 2017).

$$Resilience = \begin{cases} 100 \%, & \text{if } (Reliability = 100 \%) \\ \frac{\sum_{i=1}^{N-1} R_i}{N - \sum_{i=1}^N K_i} \times 100 \%, & \text{else} \end{cases} \quad (19)$$

$$R_i = \begin{cases} 1, & \text{if } (RAE_i > \delta \text{ and } RAE_{i+1} \leq \delta) \\ 0, & \text{else} \end{cases} \quad (20)$$

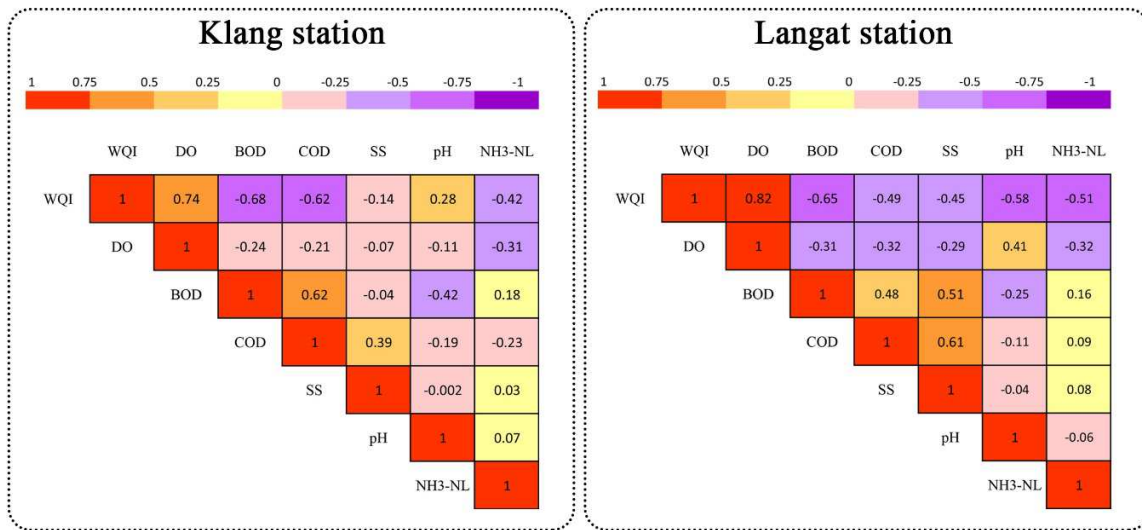
585 Where  $F_j(x)$  and  $F_{j-1}(x)$  are the CDF of  $i$  interval and the previous interval ( $i-1$ ).  $WQI_{obs}$  and  
 586  $WQI_{pre}$  denote the observed and predicted values, respectively;  $\overline{WQI_{pre}}$  is an average of  
 587 observed values, and  $N$  is the number of the dataset.  $RAE_i$  is the  $i$ th value for the data,  $K_i$  is the  
 588 number of periods that the threshold value ( $\delta$ ) of the qualified forecast is greater than or equal to  
 589 RAE value. According to the Chinese standard, the  $\delta$  is set to 20% (GB/T22482, 2008).  $R_i$  is the  
 590 number of periods in which model prediction is likely to transfer from unqualified into qualified  
 591 prediction in the  $i^{\text{th}}$  data (Rezaie-Balf et al., 2019a).

## 592 **5. Results and discussion**

593 The result section starts with the input data screening, which is finding the correlation between  
594 them, along with determining the trend following variance estimation. Then this section  
595 continuous with results of stand-alone and hybrid models for both Klang and Langat stations.  
596 The discussion part gives information about the comparison between proposed models. This  
597 section ends with the current study limitation and suggestion for future works.

### 598 **5.1. Physiochemical–covariate correlation of source data**

599 The monthly WQI co-variability with the river physiochemical parameters BOD, DO, SS, COD,  
600 NH<sub>3</sub>-NL, and pH are evaluated using the Pearson coefficient, which is known as parametric  
601 correlation analysis and primary check, in order to investigate the dependence between multiple  
602 variables at the same time. In order to assess the data relationships, the correlation factor was  
603 used in which it varies from -1 to +1, where -1 showed a negative correlation, and +1 defines  
604 positive correlation. In this study, a graphical correlation matrix is plotted to show a linear  
605 dependence between two variables for both Klang and Langat stations (Figure 5). According to  
606 this matrix, the monthly WQI has a positive, statistically significant correlation with monthly DO  
607 (0.74) and pH (0.28) for Klang and DO (0.82) for the Langat River. Also, a strong negative  
608 relationship is attained from the matrix between WQI as the corresponding target and BOD (-  
609 0.68) and COD (-0.62) for Klang, and all independent variables except DO for Langat river.



610

611 **Figure 5.** Pearson correlation matrix measures the linear relationship between each  
 612 physicochemical parameters and corresponding WQI. The color scale indicates the direction of  
 613 the correlation which means that purple color represents negatively correlated statistics, and  
 614 orange color positively correlated statistics

## 615 5.2. Monotonic trends detection of source data

616 The monotonic trends in monthly WQI are examined by a standard nonparametric method called  
 617 Spearman's rank-order correlation coefficient, denoted by  $\rho$ , to assess the fact that how two data  
 618 sets are linked to each other. In other words, the absence of trends is verified by this method in  
 619 both nonlinear and linear trends (Rezaie-Balf et al., 2019c). The null hypothesis of this analyze  
 620 the identical distribution and the independence of two variables, and the alternative hypothesis is  
 621 the existence of decreasing or increasing trends. Considering the position order for identical  
 622 values, the rank order is assigned. For instance,  $\rho$  could take -1 to +1.

623 As proven in Table 2, correlations between modeled WQI and input (physicochemical  
 624 parameters of the river) variables are estimated by the Spearman's rank correlation test for two  
 625 stations. When the P values  $<0.05$ , the confidence level for the correlation test is selected.  
 626 Spearman's rank correlation coefficients for the input variables at two stations of Klang and  
 627 Langat are more than 0.5, and the confidence level (P-values) is less than 0.05. So, the null

628 hypothesis in which the two populations are independent is rejected at a level of 5 % of  
 629 significance, and the modeled WQI is judged to be dependent on input variables.

630 **Table 2.** Values of the correlation coefficient between the WQI and the physicochemical  
 631 input variables  
 632

Station	Parameter value	Input variable					
		DO	BOD	COD	SS	pH	NH3-NL
<b>Klang</b>	R	0.73**	-0.59**	-0.78**	-0.64**	0.76**	-0.49**
	Sig	0.00	0.002	0.00	0.001	0.00	0.005
<b>Langat</b>	R	0.87**	-0.79**	-0.86**	-0.73**	0.84**	-0.69**
	Sig	0.00	0.00	0.00	0.00	0.00	0.00

633 \*\* Marked correlations are significant at  $P > 0.05$  level.  
 634

### 635 5.3. Statistical analysis of variance of source data

636 The assessment of the effects of the variables (dependent and independent) is a significant issue  
 637 in testing the data. Analysis of variance (ANOVA) is one of these tests and allows the modeler to  
 638 indicate whether independent variables have an influence or the effect of the interaction between  
 639 these variables on the dependent variable (Lam et al., 2016). The GLM-ANOVA which stands  
 640 for general linear model analysis of variance is one of the diagnostic tools and critical statistical  
 641 analysis, which reduce the error variance. In this research, the significance level of 0.05 was  
 642 utilized in order to recognize the statistical significance of physicochemical variables. These  
 643 variables, including DO, BOD, COD, SS, pH, and NH3-NL, were selected as the independent  
 644 variables in this analysis. The GLM-ANOVA was implemented on data for each variable; the  
 645 results are showed their degree of freedom, the sequential sum of squares, and their contribution  
 646 percentage of physicochemical properties at each station. The effect of the individual  
 647 independent variable on WQI (dependent variable) was valued by defining the null hypothesis of  
 648 equality of independent variances or significance test at probability level (p-values). As shown in

649 Table 3, the significance of physicochemical variables was obtained from the comparison of p-  
 650 values with the significance level factor (0.05). All of the physicochemical variables were  
 651 defined as a significant variable because of their p-value  $\leq 0.05$ . The contribution of each  
 652 physiochemical data was also shown in these two selected stations. For Klang station, NH<sub>3</sub>-NL  
 653 (90.22%) and pH (64.82%), respectively, were defined as the highest and the lowest contributors.  
 654 However, in Langat station, SS with 95.21 % and NH<sub>3</sub>-NL with 83.52 % has the highest and  
 655 lowest contribution, respectively.

656 **Table 3.** Analysis of variance (ANOVA) results for physicochemical variables of river

Station	Statistical parameters						
	Source of Variation	DF	Seq. SS	Computed F	P-value	Significance	Co. (%)
Klang	DO	227	67671.22	2.83	0.00	Yes	89.46
	BOD	33	6210.99	13.58	0.00	Yes	82.41
	COD	82	1425.42	6.6	0.00	Yes	70.99
	SS	176	17.86	1.54	0.005	Yes	88.04
	pH	140	2.57	1.41	0.017	Yes	64.82
	NH <sub>3</sub> -NL	238	93.84	2.52	0.00	Yes	90.22
	Error	13	258.02	-	-	-	-
Langat	DO	104	40865.38	1.4	0.02	Yes	87.95
	BOD	24	3141.46	14.9	0.00	Yes	79.54
	COD	50	153.43	11.26	0.00	Yes	89.5
	SS	103	33.28	2.51	0.03	Yes	95.21
	pH	93	3.672	4.01	0.00	Yes	94.19
	NH <sub>3</sub> -NL	66	29.72	3.84	0.00	Yes	83.52
	Error	116	44223	-	-	-	-

657 DF: the degree of freedom; Seq. SS: Sequential sum of squares; Co.: Contribution.

#### 658 5.4. Results for standalone and hybrid models

659 This section has highlighted the results for standalone and hybrid models in two subsections for  
 660 Klang and Langat stations in both calibration and validation stages. The initial attempt is to  
 661 investigate which training algorithm in ANN will be suitable for the given task. Besides gradient  
 662 descent that is one of the typical training algorithms, the result of another implementation with  
 663 EnKF assimilation is obtained in order to consider the effect of assimilation for predicting WQI.  
 664 Afterward, the pre-processing technique, ITD, integrating with the models mentioned above, is

665 applied in order to improve models' accuracy. Diagnostic evaluation of the statistical error  
666 metrics, including NSE, RMSE, MAE, RSD, U95, reliability, resiliency, non-parametric  
667 Kolmogorov- Smirnov (K-S) distance statistic, and visual plots such as scatter plot, time-series  
668 plot, Taylor diagram, and error bar for predicted and measured WQI are employed to assess  
669 models' performance.

670

#### 671 **5.4.1. Klang Station**

672 According to performance measures, the prediction of well-designed hybrid model ITD-EnKF-  
673 ANN vs. ITD-GD-ANN, EnKF-ANN, and GD-ANN models is numerically evaluated in this  
674 sub-section. As shown in Table 4, at the calibration stage, in terms of NSE, the accuracy of both  
675 GD-ANN and EnKF-ANN integrating the ITD approach is increased from 0.74 to 0.79 and 0.92  
676 to 0.935, respectively. By considering RMSE, the combined model errors were decreased by 45  
677 % for the ITD-GD-ANN model and 44 % for the ITD-EnKF-ANN model. In the case of MAE,  
678 ITD-EnKF-ANN (2.92) performed better than ITD-GD-ANN (3.42), and RSD explains the  
679 decrease by 0.238 and 0.206 for hybrid GD-ANN and EnKF-ANN models, respectively.  
680 Therefore, it shows the satisfactory results that hybrid models outperformed the standalone  
681 models. U95 shows that 95 % of the uncertainty confidence of the models; the results confirmed  
682 the decreasing trend in both hybrid models (ITD-GD-ANN=31.906 and ITD-EnKF-  
683 ANN=31.73). Further comparison of these models by reliability and resilience percentages  
684 showed a notable increase for both models. Focusing on K-S distance between observed and  
685 modeled WQI data, the ITD-EnKF-ANN model has the lowest amount of distance (0.068), among  
686 other models for the Klang river. This shows the preference of this model in which the observed

687 and modeled values are closer. All the above statistics show the quicker and satisfactory WQI  
 688 forecast by using ITD-GD-ANN and ITD-EnKF-ANN.

689 **Table 4.** Evaluation metrics of the proposed models in the calibration and validation stages at Klang  
 690 station

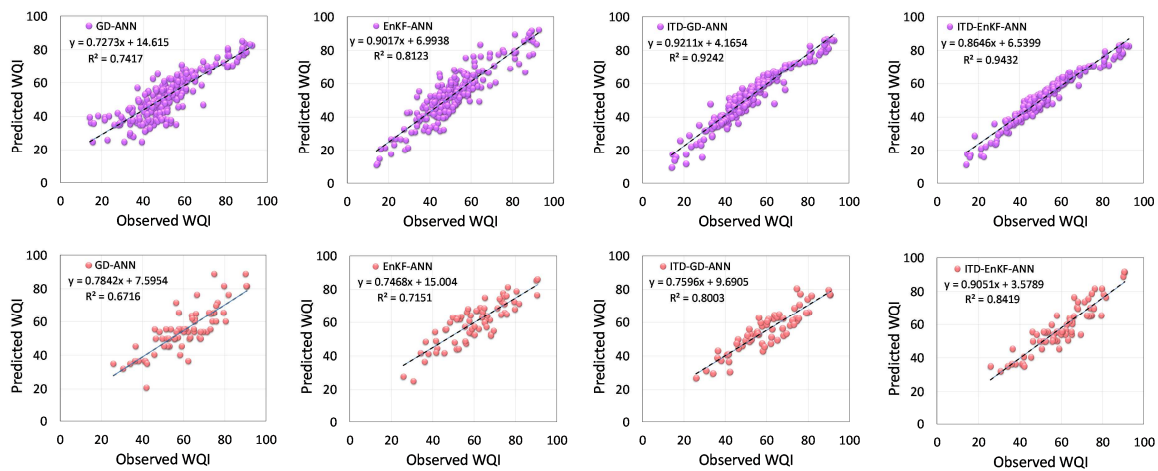
Models	Statistical error indices			
	GD-ANN	EnKF-ANN	ITD-GD-ANN	ITD-EnKF-ANN
<i>Total available data in the calibration stage</i>				
NSE	0.74	0.788	0.92	0.935
RMSE	7.97	7.21	4.31	3.97
MAE	6.23	5.704	3.42	2.92
RSD	0.508	0.459	0.27	0.253
U95	34.51	33.856	31.906	31.73
Reliability (%)	78.29	82.55	95.74	97.87
Resilience (%)	56.66	66.09	90.17	93.42
K-S distance	0.115	0.085	0.072	0.068
<i>Total available data in the validation stage</i>				
NSE	0.51	0.71	0.682	0.81
RMSE	10.05	7.66	8.055	6.17
MAE	8.16	6.51	5.97	5.069
RSD	0.69	0.532	0.559	0.42
U95	34.403	31.95	32.33	30.69
Reliability (%)	73.91	84.05	89.85	94.30
Resilience (%)	77.75	90.91	85.71	91.97
K-S distance	0.319	0.256	0.289	0.217

691  
 692  
 693 Regarding results presenting in the validation stage, all the statistical indices marked that ITD  
 694 based ANN model with the help of EnKF assimilation performed better than sole models. For  
 695 instance, the NSE increased by 0.172 and 0.1, reliability 15.94 and 10.25 and resiliency 7.96 and  
 696 1.06 for ITD-GD-ANN and ITD-EnKF-ANN respectively. The decrease in other error indices  
 697 such as RMSE, MAE also reveals that the coupled models have better results in the prediction of  
 698 WQI. In accordance with this, MAE has the highest decrease in values for both ITD-GD-ANN  
 699 (26.83 %) and ITD-EnKF-ANN (22.13 %) models, however, for RMSE values, 19.8 %, and  
 700 19.45 % deduction were noticed for coupled GD-ANN and EnKF-ANN models respectively. By  
 701 considering RSD as a mathematical index, by combining the ITD algorithm with GD-ANN, this

702 index was decreased from 0.69 to 0.559, and by combining the ITD algorithm with EnKF-ANN  
 703 models, this index decreased from 0.532 to 0.42. This shows that the error diminished, and the  
 704 prediction could be more accurate. K-S statistic in the validation stage also depicts the lowest  
 705 distance (0.217) for the ITD-EnKF-ANN method, which is the result of concordance between  
 706 input and output data of WQI.

707 The scatter plots between observed and the predicted WQI (Figure 6) reveal that at the  
 708 calibration stage, the ITD-GD-ANN model ( $R^2=0.92$ ) relatively superior to standalone GD-ANN  
 709 models ( $R^2=0.74$ ). The same results for EnKF-ANN ( $R^2=0.81$ ) as standalone and ITD-EnKF-  
 710 ANN models ( $R^2=0.94$ ) showed that combined models performed better than standalone models.  
 711 Comparison of model accuracies in the validation stage, also the priority of coupled models  
 712 (ITD-GD-ANN and ITD-EnKF-ANN), was seen. In another view of scatter plots, the regression  
 713 equation, which is based on modeled and observed values of the WQI index, is found from  
 714  $y(W_m)=aW_o+b$ .

715



716

717 **Figure 6.** Scatter plots between the observed and the predicted value of WQI for standalone and  
 718 hybrid models at Klang station in calibration (up) and validation (down) stages for all proposed  
 719 models.

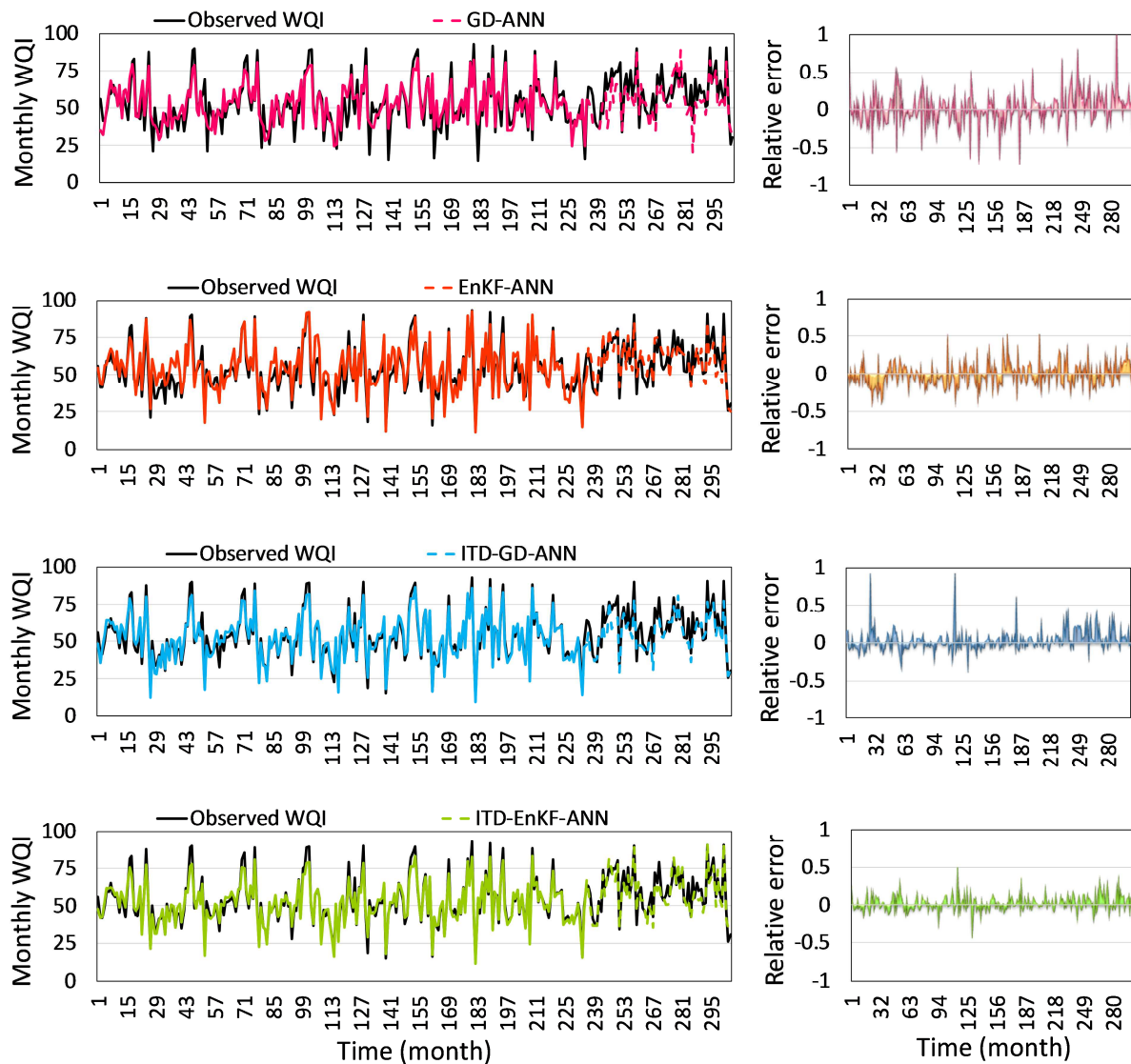
720

721 In this equation,  $W_m$  shows the modeled WQI, and  $W_o$  illustrates the observed WQI. The  
722 accurate model based on the values of  $a$ ,  $b$ , and  $R^2$  could be selected. In this research at the  
723 calibration stage, the ITD-EnKF-ANN with  $a=0.864$ ,  $b=6.5399$ , and  $R^2=0.9432$  was selected as  
724 the best model. The same analysis for the validation stage reveals that with  $a=0.9051$ ,  $b=3.5789$ ,  
725 and  $R^2=0.8419$ , the ITD-EnKF-ANN model was selected as the accurate model for predicting  
726 WQI in Klang station.

727 Although predicting all quantities of WQI is helpful for various practices, such as drinking,  
728 agriculture, and industry, the low and high values of this index are more crucial because of its  
729 direct impact on public health and the environment. In this regard, by considering time-series  
730 plots along with relative error plots which their x-axis showed their cumulative time (month) and  
731 y-axis for predicted monthly WQI high and low values of WQI, which is predicted by selected  
732 hybrid ITD-EnKF-ANN along with other models are analyzed (Figure 7).

733 Error criteria (relative error) and graphical analyses were used for evaluating the proposed  
734 methods of WQI prediction for standalone (GD-ANN and EnKF-ANN) and integrated (ITD-GD-  
735 ANN and ITD-EnKF-ANN) models. In the plots that relative error is calculated, the accuracy of  
736 models was analyzed, and it is shown that in the GD-ANN model, the peak values reach to one  
737 value, while for ITD-GD-ANN, most of the values are closer to zero. Besides, with EnKF-ANN,  
738 the error values fluctuate between 0.5 and -0.5, also in ITD-EnKF-ANN. The values of relative  
739 error were close to zero, and the fluctuations are extremely low. Considering time series plots  
740 and relative error plots, ITD-EnKF-ANN was found to be more suitable for WQI prediction.  
741 However, ANN, with the help of the GD algorithm, had poor accuracy and was not a reliable  
742 model.

743



744

745 **Figure 7.** The hydrographs of observed vs. predicted monthly WQI using standalone and hybrid  
 746 models for calibration (solid line) and validation (dash line) stages and relative error plot for  
 747 Klang station.

748

#### 749 5.4.2. Langat Station

750 Similar to the previous section, Table 5 exhibits the mathematical indexes in the calibration stage  
 751 and validation stages for proposed models. As shown in the calibration stage, NSE value was

752 increased from 0.82 to 0.89 in ITD-GD-ANN and 0.87 to 0.92 in ITD-EnKF-ANN in comparison  
 753 with their sole-models. The error values of RMSE, MAE, and RSD were decreased by 22 %, 25  
 754 %, 24 % when the GD-ANN model was combined with ITD algorithms. By comparing the  
 755 uncertainty of models, ITD-EnKF-ANN (U95=41.75) performed better than ITD-GD-ANN  
 756 (U95=42.38) at 95 % of confidence. In the validation stage, the same indices provide adequate  
 757 proof that combines ITD-EnKF-ANN outperformed the ITD-GD-ANN models. For example,  
 758 considering NSE, it is increased by 1.328 for the GD-ANN model also 0.14 for the EnKF-ANN  
 759 model by a combination of ITD algorithms. By considering the error indices, RMSE, MAE, RSD  
 760 were decreased by their values in coupled ITD models. In the other aspect, the lowest difference  
 761 between two consecutive cumulative distribution functions (CDF) of input and output WQI data  
 762 in the calibration stage for Langat station is 0.106, which is belong for ITD-EnKF-ANN model.  
 763 This shows that the hybrid ITD-EnKF-ANN model performed better than the other models. The  
 764 same outcome of the preference of the ITD-EnKF-ANN model with a distance of 0.217 was  
 765 calculated for the validation stage. These results reveal that the ITD algorithm as a pre-  
 766 processing algorithm performed better while combining to DDMs.

767 **Table 5.** Evaluation metrics of the proposed models in the calibration and validation stages at Langat  
 768 station

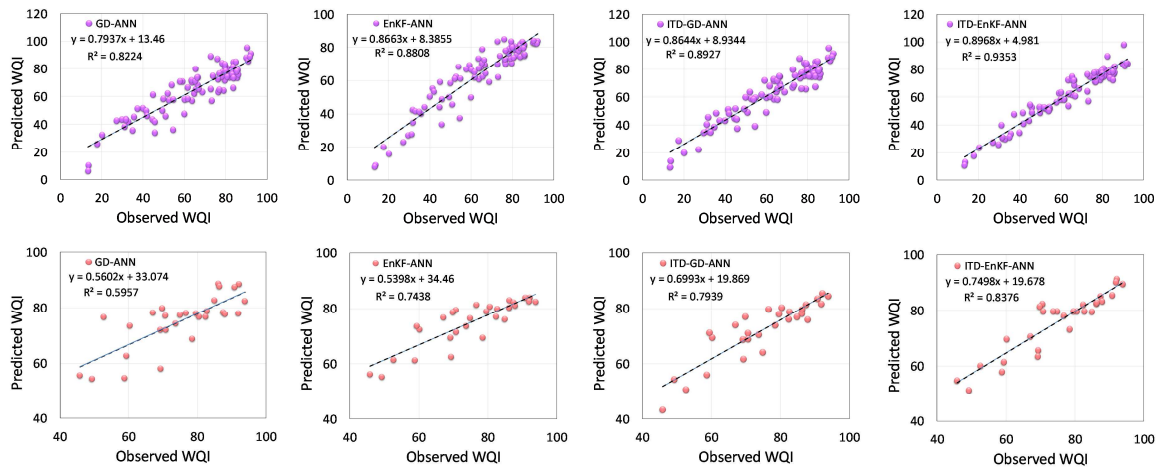
Models	Statistical error indices			
	GD-ANN	EnKF-ANN	ITD-GD-ANN	ITD-EnKF-ANN
<i>Total available data in the calibration stage</i>				
NSE	0.82	0.87	0.89	0.92
RMSE	8.66	7.09	6.74	5.61
MAE	7.21	5.91	5.42	4.59
RSD	0.42	0.345	0.32	0.27
U95	43.71	42.607	42.38	41.75
Reliability (%)	72.73	86.36	89.77	95.45
Resilience (%)	66.49	83.33	77.78	89.56
K-S distance	0.159	0.148	0.125	0.106
<i>Total available data in the validation stage</i>				
NSE	0.598	0.69	0.73	0.83
RMSE	8.28	7.27	6.69	5.403

MAE	6.504	6.16	5.72	4.38
RSD	0.622	0.54	0.503	0.406
U95	30.72	29.72	29.19	28.15
Reliability (%)	89.65	89.65	94.55	97.68
Resilience (%)	67.58	67.58	91.48	94.15
K-S distance	0.310	0.276	0.241	0.217

769

770

771 Figure 8 showed the scatter plot of the proposed models in order to assess the best accuracy for  
 772 WQI prediction. Considering Figure 8 in detail, at the calibration stage, the correlation  
 773 coefficient for ITD-GD-ANN was increased by 0.07 in comparison with stand-alone GD-ANN.  
 774 Also, the coefficient of determination for ITD-EnKF-ANN increased by 0.09 compared with  
 775 stand-alone EnKF-ANN. In the validation stage, the  $R^2$  for ITD-GD-ANN and ITD-EnKF-ANN  
 776 were increased by 25 % and 11 % in comparison with their sole models. The outcomes from the  
 777 stand-alone and combined models reveal that in both calibration and validation stages, the ITD-  
 778 EnKF-ANN was confirmed the best model in WQI prediction.



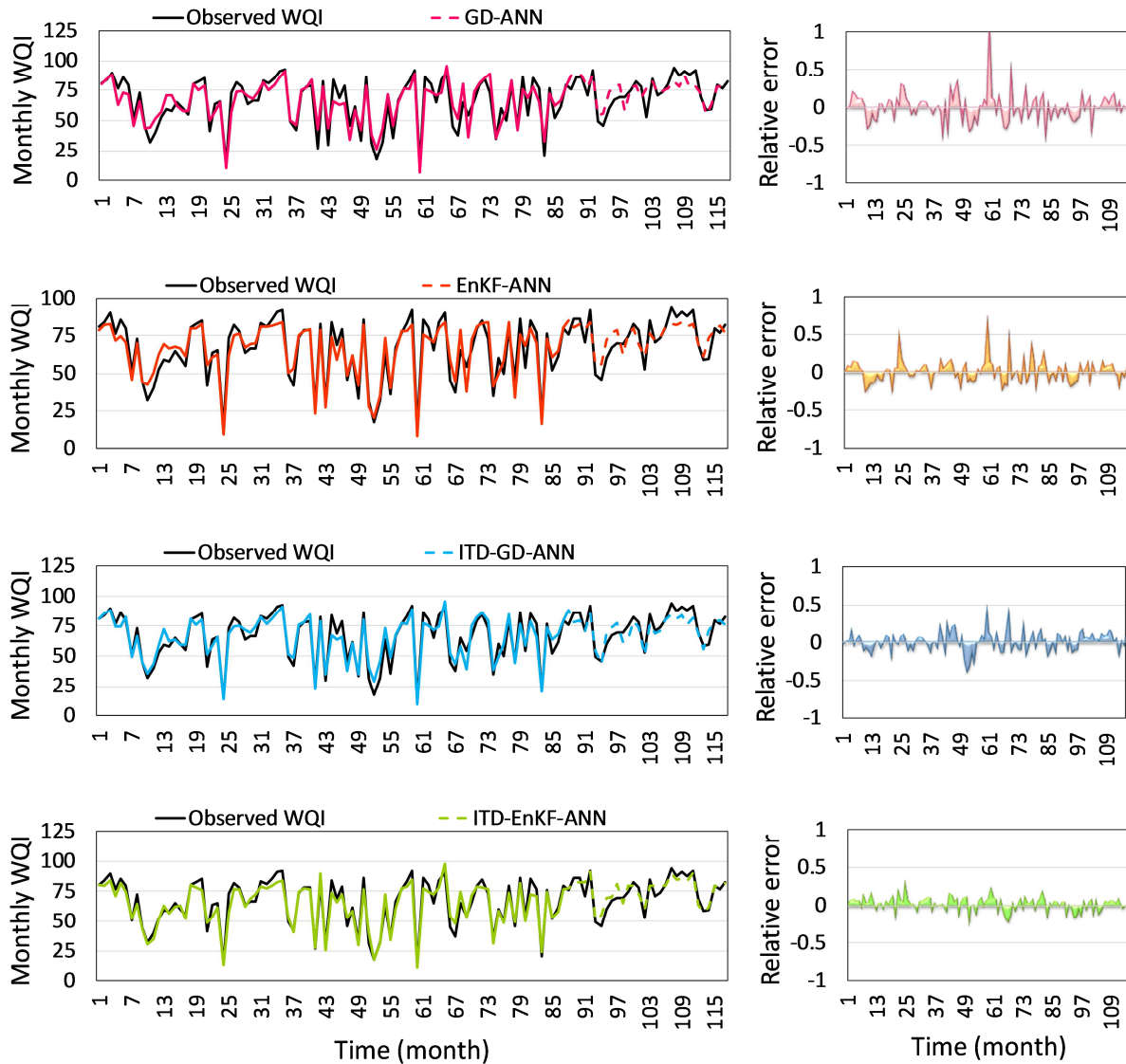
779

780 **Figure 8.** Scatter plots between the observed and the predicted value of WQI for standalone and  
 781 hybrid models at Langat station in calibration (upper row) and validation (lower row) stages for  
 782 all proposed models.

783

784 Figure 9 depicts the time series of predicted vs. observed values of WQI calibration and  
785 validation stages. In standalone GD-ANN and EnKF-ANN models, the maximum value of  
786 relative error belongs to 61<sup>st</sup> month with RE=1 and RE=0.7, respectively. By comparing the two  
787 combined models, ITD-GD-ANN and ITD-EnKF-ANN, it is shown that the maximum value for  
788 relative error was between 0.5 and -0.5, and the error values are close to zero in ITD-EnKF-ANN  
789 model. Thus, this also reaffirms that the ITD-EnKF-ANN hybrid model has better predictive  
790 skill than the other combined and standalone models considered in this research.  
791 Furthermore, the utilization of such a modeling procedure does not only predict water quality  
792 index accurately but also can improve the water quality monitoring programs by reducing the  
793 costly experimental testing and time-consuming issues.

794



795

796 **Figure 9.** The hydrographs of observed vs. predicted monthly WQI using standalone and hybrid  
 797 models for calibration (solid line) and validation (dash line) stages and relative error plot for  
 798 Langat station.

### 799 5.5. Further comparison among proposed models

800 Based on peak values of predicted monthly WQI with the observed extreme values of each  
 801 station, the best models can be identified. For this aim, Table 6 demonstrates the ten highest  
 802 extreme values of predicted WQI for two stations considering the GD-ANN, EnKF-ANN, ITD-  
 803 GD-ANN, and ITD-EnKF-ANN models. As shown in Table 6, the maximum difference between  
 804 the extreme value belongs to the EnKF-ANN model while the minimum difference goes to ITD-

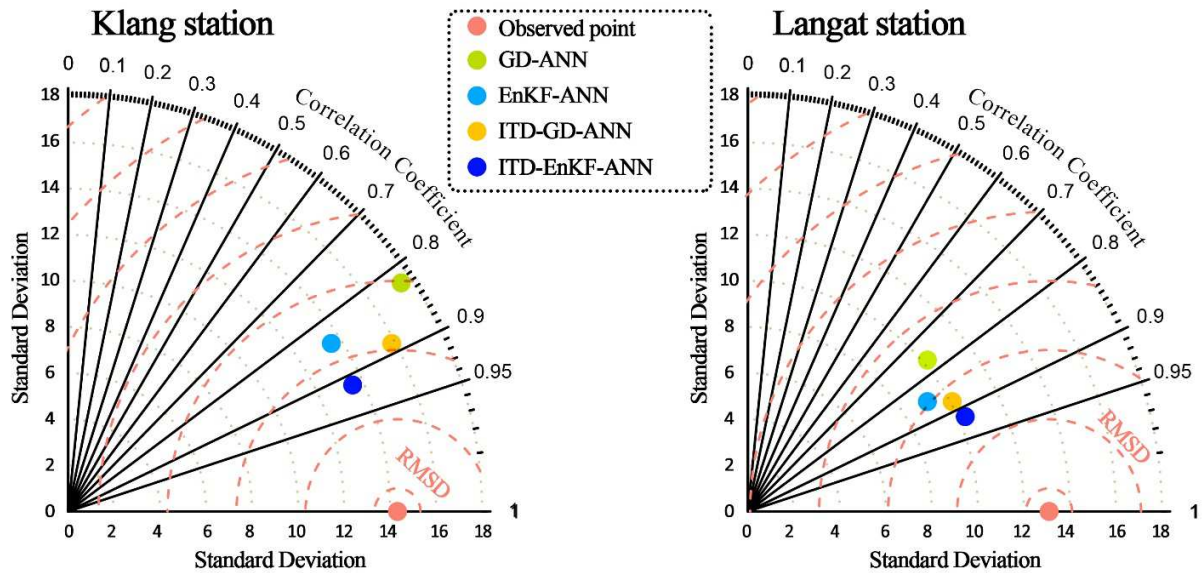
805 EnKF-ANN for Klang station. Again for Langat station, the highest value for WQI observation  
 806 was 93.84, while the peak values for the models were 82.506, 82.436, 84.484, and 89.538 for  
 807 GD-ANN, EnKF-ANN, ITD-GD-ANN, and ITD-EnKF-ANN models, respectively. This  
 808 resulted that the ITD-EnKF-ANN model outperformed other models in the view of extreme  
 809 values.

810 **Table 6:** Accuracy evaluation of different models for predicting extreme WQI values (Klang and  
 811 Langat stations)

Observed value	GD-ANN	EnKF-ANN	ITD-GD-ANN	ITD-EnKF-ANN
<i>Klang station</i>				
92.86	88.252	82.528	85.916	90.471
91.77	83.628	83.134	86.181	92.699
90.78	86.110	81.664	76.881	91.664
90.15	76.608	81.664	77.14	91.664
90.13	85.3826	88.766	81.499	88.766
90.12	85.139	78.468	81.283	88.431
89.87	77.866	78.892	81.306	78.006
89.42	91.660	79.195	82.079	89.152
89.30	87.959	83.68	86.561	83.098
89.00	87.207	80.529	84.054	86.649
<i>Langat station</i>				
93.84	82.506	82.436	84.484	89.538
92.2	91.099	83.838	91.389	86.101
92.12	88.549	83.980	85.437	91.274
91.85	77.995	82.551	81.692	90.269
91.71	86.74	82.248	89.072	86.618
90.91	84.721	82.452	86.299	85.442
90.83	84.5	83.960	83.497	86.411
90.37	95.478	84.063	95.396	92.93
89.93	87.006	82.896	88.47	86.262
87.90	77.701	81.121	79.935	83.305

812  
 813 Figure 10 demonstrates the Taylor diagram, which is used to quantify the degree of  
 814 correspondence between modeled and observed WQI in the tested data in terms of three primary  
 815 statistics on a single diagram. It shows the RMSE, the correlation coefficient, and the standard  
 816 deviation for GD-ANN, EnKF-ANN, ITD-GD-ANN, and ITD-EnKF-ANN models for both  
 817 Klang and Langat stations.

818



819

820 **Figure 10.** Taylor plots indicating the correlation coefficient and standard deviation in the  
 821 validation stage based on the standalone models vs. the hybrid-assimilated models for predicting  
 822 monthly water quality index at two candidate study stations.

823

824 Concurring with earlier results, it was evident that the ITD-EnKF-ANN model in both stations is  
 825 closer to the optimum reference point when a combined visual valuation of the statistics is made.  
 826 As evident from this diagram, the coupled ITD-EnKF-ANN model has a higher correlation and  
 827 inversely a lower standard deviation for both stations in the prediction of WQI. However, the  
 828 GD-ANN model lies much farther to the line representing the centered root-mean-square  
 829 difference, while the standard deviation of the GD-ANN model remains modestly farther than  
 830 other models to reference.

831 The empirical cumulative distribution function (ECDF) was plotted at different predicting  
 832 abilities (Figure 11), which predicted error of monthly WQI in the x-axis and the percentage of  
 833 the distribution function in the y-axis for each model. According to the plot, it is evident that the

834 ITD-EnKF-ANN hybrid model was gently better than ITD-GD-ANN for WQI predicting at both  
835 stations, and both decomposed-based models were superior to the original models.

836 Based on the percentage of errors in the minimum error bracket (i.e., from 0 to 5) for the Langat  
837 station clearly confirms that the ITD-EnKF-ANN was the most responsive model in predicting  
838 water quality index (50 %) compared to 44 % for the ITD-EnKF-ANN, 36 % for the EnKF-  
839 ANN, and 29 % for the standalone GD-ANN model. Inferior performances were demonstrated  
840 when the non-ITD/DA mechanisms were utilized. Therefore, the highest performance with the  
841 lowest predicted error resulted from the GD-ANN model. The results of these ECDF plots are  
842 consistent with the subject that WQI prediction has a better result when using an ensemble  
843 Kalman filter ANN model, which is combined with ITD pre-processing techniques.

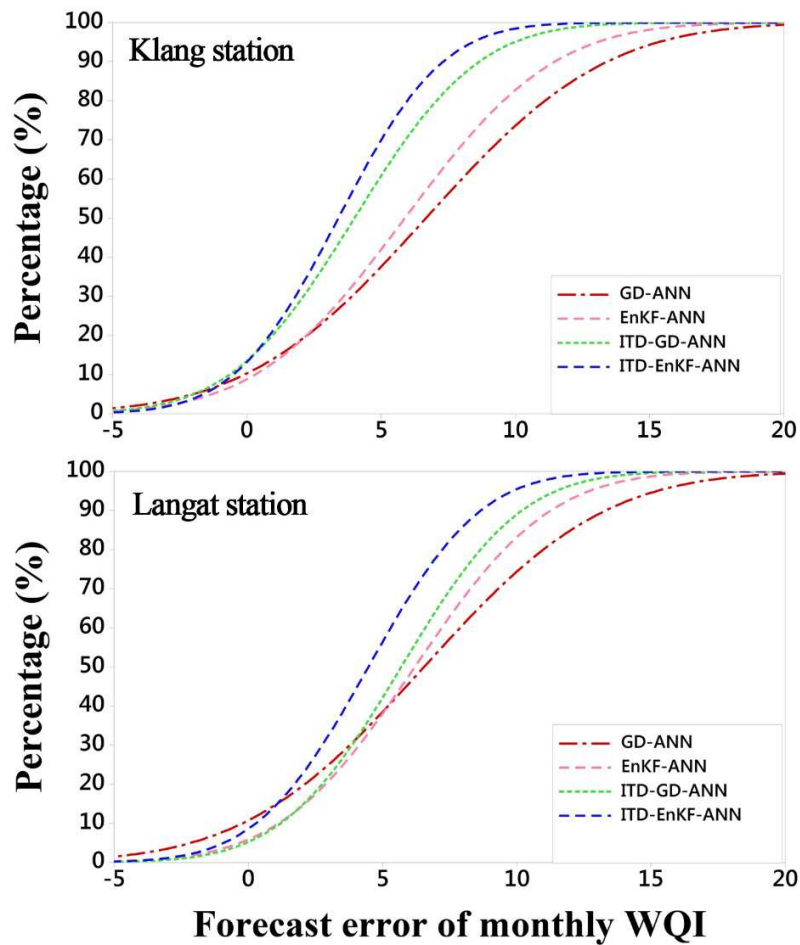
844

845

846

847

848



849

850 **Figure 11.** Empirical cumulative distribution (ECDF) of the absolute forecasted error  $|FE|$  for the  
 851 ITD-EnKF-ANN model compared to the other models at Klang and Langat stations in the  
 852 validation phase.

853

### 854 5.6. Current study limitations

855 This study consistent with the concept of water quality index modeling by using neural networks  
 856 modeling, which is used the ITD pre-processing data algorithm for the first time. Despite using a  
 857 standard training algorithm, namely gradient descent in this research, ensemble Kalman filter  
 858 algorithm as an assimilation algorithm used in this research in order to eliminate GD algorithm  
 859 drawbacks for improving the model's accuracy in terms of prediction. For more satisfaction on

860 the result of WQI prediction, data decomposition technique, ITD, proposed to extract  
861 input/output variables into different sub-signals in order to overcome the non-stationarity  
862 features in the time series real data.

863 The present study has shortcomings that create an opportunity for follow-up research in the field  
864 of hydrology. Implementation of the ITD pre-processing technique integrated with EnKF-ANN  
865 is time-consuming because it produces a large number of PRCs. Follow-up studies can consider  
866 another pre-processing method to reduce computational cost or to implement ITD-EnKF-ANN  
867 all together in one main source code, at least to reduce the time of development. Another  
868 limitation through the study was the lack of meteorological data in some months for both  
869 stations, and this drawback may provide uncertainty on the prediction of water quality index. In  
870 this regard, it is suggested that future studies might use the satellite-based dataset in order to  
871 analyze the data for WQI prediction. In addition, as mentioned above, source data was limited in  
872 terms of predicting WQI and was the three-month timescale. Hence, a follow-up study could  
873 investigate the model's skill for better temporal resolution (e.g., hourly, daily, weekly, and  
874 monthly) with satellite-based prediction.

875

## 876 **6. Conclusions**

877 This paper underlined the importance of water quality modeling for human health. In this study,  
878 as the first step, a comprehensive literature review was carried out on the current state of river  
879 WQI modeling. It was found that pH and DO as the physicochemical parameters with the 95.83  
880 and 91.67, respectively, were the most influential parameters researchers considered for the  
881 studies.

882 Besides the GD algorithm that was initially used for finding the minimum of a function in ANN,  
883 the Ensemble Kalan Filter (EnKF) assimilation approach that is one of the best solutions to  
884 nonlinear problems, is used to merge ANN model prediction with assimilating production data at  
885 two famous polluted rivers in Malaysia, namely Klang and Langat. Considering evaluation  
886 metrics, using EnKF to predict WQI could improve the accuracy of the standalone ANN model  
887 by 39 % and 17 %, respectively, for Klang and Langat stations in terms of NSE compared with  
888 GD training algorithms. In addition, predicting error was reduced to 7.66 and 6.51 in terms of  
889 RMSE and MAE, respectively, by augmenting the state space with model parameters (using DA  
890 technique) compared to no assimilation at Klang station.

891 As a further attempt, the performance of a newly constructed ensemble hybrid decomposition  
892 model embedded with the Intrinsic Time-scale Decomposition (ITD) as a pre-processing  
893 technique integrated with the ANN model was adopted. That is, the physicochemical time series  
894 and the corresponding target using the ITD algorithm were extracted (decomposed), resulting in  
895 improved performance of the standalone models. In this respect, the RSD and U95 values of the  
896 ITD-EnKF-ANN model for WQI estimation were reduced to 25.3 % and 5.2 %, respectively,  
897 compared with the EnKF-ANN model at Langat station. Considering the plotted empirical  
898 cumulative distribution function (ECDF) at different predicting abilities in both stages of  
899 calibration and validation along with non-parametric statistics, namely Kolmogorov-Smirnov (K-  
900 S) Distance method in Klang and Langat rivers, the hybrid assimilated ITD-EnKF-ANN  
901 performed better than the other models.

902 Overall, the achieved results indicated that the hybrid assimilated ITD-EnKF-ANN model would  
903 be a robust approach to predict WQI on the monthly timescale since the results were favorable  
904 for both Malaysian stations. It is also can be proposed as a possible solution in order to reduce

905 the noise in highly nonlinear hydrological phenomena such as the prediction of streamflow, solar  
906 radiation, etc.

907 In order to widen the scope of the study, the ITD-EnKF-ANN model could be improved with  
908 ensemble-based uncertainty testing via a bootstrapping and the Bayesian model averaging  
909 techniques, although the proposed model had a precise prediction. One possibility for future  
910 study is to consider other DDMs such as gene expression programming, extreme learning  
911 machine, etc. for integrating with ensemble Kalman filter to perform an accurate model in the  
912 prediction of the hydrological processes (i.e., streamflow, rainfall, water stage, groundwater,  
913 etc.).

914 With the aim of the accuracy of WQI modeling, it is better to consider more data samples and  
915 various input variables such as heavy metals, pollutants, and radioactive samples from different  
916 rivers in Malaysia. The water quality can also be affected by their background basin, so this can  
917 affect the concentration of each quality parameter. Thus, for future works, the authors suggested  
918 assessing basin effects too. Finally, it can be suggested as a potential alternative to enhance the  
919 forecasting accuracy using other pre-processing approaches, complete ensemble local mean  
920 decomposition with adaptive noise, variational mode decomposition, complete ensemble  
921 empirical mode decomposition(CEEMD), improved CEEMD, local mean decomposition  
922 (LMD), and ensemble LMD.

## 923 Acknowledgments

924 The authors appreciate so much the facilities support by the Civil Engineering Department,  
 925 Faculty of Engineering, University of Malaya, Malaysia, and the financial support received from  
 926 research grant coded GPF082A-2018 funded by the University of Malaya and 2020106TELCO  
 927 grant by the Innovation & Research Management Center (iRMC), Universiti Tenaga Nasional  
 928 (UNITEN) and Telkom University, Indonesia. Besides, the authors would like to thank the  
 929 Department of Environment (DoE) for providing data and technical support.

930 **References**

- 931 Abbaszadeh, P., Moradkhani, H., Yan, H., 2017. Enhancing hydrologic data assimilation by  
 932 evolutionary Particle Filter and Markov Chain Monte Carlo. *Adv. Water Resour.*  
 933 <https://doi.org/10.1016/j.advwatres.2017.11.011>
- 934 Ahmad, Z., Rahim, N.A., Bahadori, A., Zhang, J., 2017. Improving water quality index  
 935 prediction in Perak River basin Malaysia through a combination of multiple neural  
 936 networks. *Int. J. River Basin Manag.* 15, 79–87.  
 937 <https://doi.org/10.1080/15715124.2016.1256297>
- 938 Ahmed, A.N., Hayder, G., Rahman, R.A.B.A., Borhana, A.A., 2019. Rainfall-runoff forecasting  
 939 utilizing genetic programming technique. *Int. J. Civ. Eng. Technol.* 10, 1523–1534.
- 940 Al-Musawi, N., Al-Rubaie, F.M., Al-Musawi, N.O., 2017. prediction and assessment of water  
 941 quality index using neural network model and gis case study: tigris river in baghdad city  
 942 chlorine decay view project prediction and assessment of water quality index using neural  
 943 network model and gis case study AND GIS. *Appl. Res. J.* 3, 343–353.
- 944 Amornsamankul, S., Road, S.A., Road, S.A., Road, S.A., n.d. Modified WQI Model using  
 945 Fourier series and Genetic Algorithm Technique. *Recent Res. Autom. Control Electron.*  
 946 *Modif.* 73–76.
- 947 Attar, N.F., Khalili, K., Behmanesh, J., Khanmohammadi, N., 2018. On the reliability of soft  
 948 computing methods in the estimation of dew point temperature: The case of arid regions of  
 949 Iran. *Comput. Electron. Agric.* 153, 334–346. <https://doi.org/10.1016/j.compag.2018.08.029>
- 950 Attar, N.F., Pham, Q.B., Nowbandegani, S.F., Rezaie-Balf, M., Fai, C.M., Ahmed, A.N.,  
 951 Pipelzadeh, S., Dung, T.D., Nhi, P.T.T., Khoi, D.N., El-Shafie, A., 2020. Enhancing the  
 952 Prediction Accuracy of Data-Driven Models for Monthly Streamflow in Urmia Lake Basin  
 953 Based upon the Autoregressive Conditionally Heteroskedastic Time-Series Model. *Appl.*  
 954 *Sci.* 10, 571. <https://doi.org/10.3390/app10020571>
- 955 Babaei, S., F, Hassani, A H, Torabian, A, Karbassi, A R, Hosseinzadeh, L., F, 2011. Water  
 956 quality index development using fuzzy logic: A case study of the Karoon River of Iran.  
 957 *African J. Biotechnol.* 10, 10125–10133. <https://doi.org/10.5897/AJB11.1608>
- 958 Babbar, R., Babbar, S., 2017. Predicting river water quality index using data mining techniques.  
 959 *Environ. Earth Sci.* 76. <https://doi.org/10.1007/s12665-017-6845-9>

- 960 Bagheri, M., Mirbagheri, S.A., Bagheri, Z., Kamarkhani, A.M., 2015. Modeling and  
 961 optimization of activated sludge bulking for a real wastewater treatment plant using hybrid  
 962 artificial neural networks-genetic algorithm approach. *Process Saf. Environ. Prot.* 95, 12–  
 963 25. <https://doi.org/10.1016/J.PSEP.2015.02.008>
- 964 Chang, N. Bin, Chen, H.W., Ning, S.K., 2001. Identification of river water quality using the  
 965 fuzzy synthetic evaluation approach. *J. Environ. Manage.* 63, 293–305.  
 966 <https://doi.org/10.1006/jema.2001.0483>
- 967 Chau, K., 2006. A review on integration of artificial intelligence into water quality modelling.  
 968 *Mar. Pollut. Bull.* 52, 726–733. <https://doi.org/10.1016/J.MARPOLBUL.2006.04.003>
- 969 Clark, M.P., Rupp, D.E., Woods, R.A., Zheng, X., Ibbitt, R.P., Slater, A.G., Schmidt, J.,  
 970 Uddstrom, M.J., 2008. Hydrological data assimilation with the ensemble Kalman filter: Use  
 971 of streamflow observations to update states in a distributed hydrological model. *Adv. Water*  
 972 *Resour.* 31, 1309–1324. <https://doi.org/10.1016/J.ADVWATRES.2008.06.005>
- 973 DOE, 2007. Malaysia Environmental Quality Report. Malaysia Env. Rep.1–86.
- 974 Dong, X., Lian, J., Wang, H., 2019. Vibration source identification of offshore wind turbine  
 975 structure based on optimized spectral kurtosis and ensemble empirical mode decomposition.  
 976 *Ocean Eng.* 172, 199–212. <https://doi.org/10.1016/j.oceaneng.2018.11.030>
- 977 El-Kowrany, S.I., El-Zamarany, E.A., El-Nouby, K.A., El-Mehy, D.A., Abo Ali, E.A., Othman,  
 978 A.A., Salah, W., El-Ebiary, A.A., 2016. Water pollution in the Middle Nile Delta, Egypt:  
 979 An environmental study. *J. Adv. Res.* 7, 781–794.  
 980 <https://doi.org/10.1016/J.JARE.2015.11.005>
- 981 Evensen, G., 1994. Sequential data assimilation with a nonlinear quasi-geostrophic model using  
 982 Monte Carlo methods to forecast error statistics. *J. Geophys. Res.* 99.
- 983 Fijani, E., Barzegar, R., Deo, R., Tziritis, E., Skordas, K., 2019. Design and implementation of a  
 984 hybrid model based on two-layer decomposition method coupled with extreme learning  
 985 machines to support real-time environmental monitoring of water quality parameters. *Sci.*  
 986 *Total Environ.* 648, 839–853. <https://doi.org/10.1016/J.SCITOTENV.2018.08.221>
- 987 Frei, M.G., Osorio, I., 2007. Intrinsic time-scale decomposition: time–frequency–energy analysis  
 988 and real-time filtering of non-stationary signals. *Proc. R. Soc. A Math. Phys. Eng. Sci.* 463,  
 989 321–342. <https://doi.org/10.1098/rspa.2006.1761>
- 990 Gaafar, M., Mahmoud, S.H., Gan, T.Y., Davies, E.G.R., 2019. A practical GIS-based hazard  
 991 assessment framework for water quality in stormwater systems. *J. Clean. Prod.*  
 992 <https://doi.org/10.1016/j.jclepro.2019.118855>
- 993 Gazzaz, N.M., Yusoff, M.K., Aris, A.Z., Juahir, H., Ramli, M.F., 2012. Artificial neural network  
 994 modeling of the water quality index for Kinta River (Malaysia) using water quality  
 995 variables as predictors. *Mar. Pollut. Bull.* 64, 2409–2420.  
 996 <https://doi.org/10.1016/j.marpolbul.2012.08.005>
- 997 Gazzaz, N.M., Yusoff, M.K., Ramli, M.F., Juahir, H., Aris, A.Z., 2015. Artificial Neural  
 998 Network Modeling of the Water Quality Index Using Land Use Areas as Predictors. *Water*  
 999 *Environ. Res.* 87, 99–112. <https://doi.org/10.2175/106143014X14062131179276>
- 1000 GB/T22482-2008, n.d. GB/T 22482-2008 - Standard for hydrological information and  
 1001 hydrological forecasting (TEXT OF DOCUMENT IS IN CHINESE) [WWW Document].  
 1002 URL <https://webstore.ansi.org/standards/spc/gb224822008> (accessed 3.23.20).
- 1003 Gurjar, S.K., Tare, V., 2019. Spatial-temporal assessment of water quality and assimilative  
 1004 capacity of river Ramganga, a tributary of Ganga using multivariate analysis and QUEL2K.  
 1005 *J. Clean. Prod.* 222, 550–564. <https://doi.org/10.1016/j.jclepro.2019.03.064>

- 1006 Hameed, M., Sharqi, S.S., Yaseen, Z.M., Afan, H.A., Hussain, A., Elshafie, A., 2017.  
1007 Application of artificial intelligence (AI) techniques in water quality index prediction: a  
1008 case study in tropical region, Malaysia. *Neural Comput. Appl.* 28, 893–905.  
1009 <https://doi.org/10.1007/s00521-016-2404-7>
- 1010 Ho, J.Y., Afan, H.A., El-Shafie, A.H., Koting, S.B., Mohd, N.S., Jaafar, W.Z.B., Lai Sai, H.,  
1011 Malek, M.A., Ahmed, A.N., Mohtar, W.H.M.W., Elshorbagy, A., El-Shafie, A., 2019a.  
1012 Towards a time and cost effective approach to water quality index class prediction. *J.*  
1013 *Hydrol.* 575, 148–165. <https://doi.org/10.1016/j.jhydrol.2019.05.016>
- 1014 Ho, J.Y., Afan, H.A., El-Shafie, A.H., Koting, S.B., Mohd, N.S., Jaafar, W.Z.B., Lai Sai, H.,  
1015 Malek, M.A., Ahmed, A.N., Mohtar, W.H.M.W., Elshorbagy, A., El-Shafie, A., 2019b.  
1016 Towards a time and cost effective approach to water quality index class prediction. *J.*  
1017 *Hydrol.* 575, 148–165. <https://doi.org/10.1016/j.jhydrol.2019.05.016>
- 1018 Hore, A., Dutta, S., Datta, S., Bhattacharjee, C., 2008. Application of an artificial neural network  
1019 in wastewater quality monitoring: prediction of water quality index. *Int. J. Nucl. Desalin.* 3,  
1020 160. <https://doi.org/10.1504/IJND.2008.020223>
- 1021 Ishikawa, Y., Murata, M., Kawaguchi, T., 2019. Globally applicable water quality simulation  
1022 model for river basin chemical risk assessment. *J. Clean. Prod.* 239.  
1023 <https://doi.org/10.1016/j.jclepro.2019.118027>
- 1024 Johns, C.J., Mandel, J., 2008. A two-stage ensemble Kalman filter for smooth data assimilation.  
1025 *Environ. Ecol. Stat.* 15, 101–110. <https://doi.org/10.1007/s10651-007-0033-0>
- 1026 Juahir, H., Zain, S.M., Toriman, M.E., Mokhtar, M., Man, H.C., 2004. Application of Artificial  
1027 Neural Network Models for Prediction Water Quality Index. *Quality* 16, 42–55.
- 1028 Justel, A., Peña, D., Zamar, R., 1997. A multivariate Kolmogorov-Smirnov test of goodness of  
1029 fit. *Stat. Probab. Lett.* 35, 251–259. [https://doi.org/10.1016/s0167-7152\(97\)00020-5](https://doi.org/10.1016/s0167-7152(97)00020-5)
- 1030 Kadam, A.K., Wagh, V.M., Muley, A.A., Umrikar, B.N., Sankhua, R.N., 2019. Prediction of  
1031 water quality index using artificial neural network and multiple linear regression modelling  
1032 approach in Shivganga River basin, India. *Model. Earth Syst. Environ.* 1–12.  
1033 <https://doi.org/10.1007/s40808-019-00581-3>
- 1034 Kalman, R.E., 1960. A New Approach to Linear Filtering and Prediction Problems. *J. Basic Eng.*  
1035 82, 35. <https://doi.org/10.1115/1.3662552>
- 1036 Karunasingha, D.S.K., Liong, S.-Y., 2018. Enhancement of chaotic hydrological time series  
1037 prediction with real-time noise reduction using Extended Kalman Filter. *J. Hydrol.* 565,  
1038 737–746. <https://doi.org/10.1016/J.JHYDROL.2018.08.044>
- 1039 Kashif Gill, M., Kemblowski, M.W., McKee, M., 2007. Soil Moisture Data Assimilation Using  
1040 Support Vector Machines and Ensemble Kalman Filter. *J. Am. Water Resour. Assoc.* 43,  
1041 1004–1015. <https://doi.org/10.1111/j.1752-1688.2007.00082.x>
- 1042 Khalid, Samina, Murtaza, B., Shaheen, I., Ahmad, I., Ullah, M.I., Abbas, T., Rehman, F., Ashraf,  
1043 M.R., Khalid, Sana, Abbas, S., Imran, M., 2018. Assessment and public perception of  
1044 drinking water quality and safety in district Vehari, Punjab, Pakistan. *J. Clean. Prod.* 181,  
1045 224–234. <https://doi.org/10.1016/j.jclepro.2018.01.178>
- 1046 Khan, F., Husain, T., Lumb, A., 2003. Water Quality Evaluation and Trend Analysis in Selected  
1047 Watersheds of the Atlantic Region of Canada. *Environ. Monit. Assess.* 88, 221–248.  
1048 <https://doi.org/10.1023/A:1025573108513>
- 1049 Khuan, L.Y., Hamzah, N., Jailani, R., 2002. Prediction of water quality index (WQI) based on  
1050 artificial neural network (ANN). 2002 Student Conf. Res. Dev. Glob. Res. Dev. Electr.  
1051 *Electron. Eng. SCORED 2002 - Proc.* 157–161.

- 1052 <https://doi.org/10.1109/SCORED.2002.1033081>
- 1053 Kisi, O., Yaseen, Z.M., 2019. The potential of hybrid evolutionary fuzzy intelligence model for  
1054 suspended sediment concentration prediction. *Catena* 174, 11–23.  
1055 <https://doi.org/10.1016/j.catena.2018.10.047>
- 1056 Kükreçer, S., Mutlu, E., 2019. Assessment of surface water quality using water quality index and  
1057 multivariate statistical analyses in Saraydüzü Dam Lake, Turkey. *Environ. Monit. Assess.*  
1058 191. <https://doi.org/10.1007/s10661-019-7197-6>
- 1059 Kumar, B., Singh, U.K., Ojha, S.N., 2019. Evaluation of geochemical data of Yamuna River  
1060 using WQI and multivariate statistical analyses: a case study. *Int. J. River Basin Manag.* 17,  
1061 143–155. <https://doi.org/10.1080/15715124.2018.1437743>
- 1062 Lam, T.C., Ge, H., Fazio, P., 2016. Energy positive curtain wall configurations for a cold climate  
1063 using the Analysis of Variance (ANOVA) approach. *Build. Simul.* 9, 297–310.  
1064 <https://doi.org/10.1007/s12273-016-0275-6>
- 1065 Leong, W.C., Bahadori, A., Zhang, J., Ahmad, Z., 2019. Prediction of water quality index (WQI)  
1066 using support vector machine (SVM) and least square-support vector machine (LS-SVM).  
1067 *Int. J. River Basin Manag.* 0, 1–8. <https://doi.org/10.1080/15715124.2019.1628030>
- 1068 Lermontov, A., Yokoyama, L., Lermontov, M., Machado, M.A.S., 2009. River quality analysis  
1069 using fuzzy water quality index: Ribeira do Iguape river watershed, Brazil. *Ecol. Indic.* 9,  
1070 1188–1197. <https://doi.org/10.1016/j.ecolind.2009.02.006>
- 1071 Li, S., Gu, S., Tan, X., Zhang, Q., 2009. Water quality in the upper Han River basin, China: The  
1072 impacts of land use/land cover in riparian buffer zone. *J. Hazard. Mater.* 165, 317–324.  
1073 <https://doi.org/10.1016/j.jhazmat.2008.09.123>
- 1074 Liou, S.-M., Lo, S.-L., Wang, S.-H., 2004. A Generalized Water Quality Index for Taiwan.  
1075 *Environ. Monit. Assess.* 96, 35–52. <https://doi.org/10.1023/B:EMAS.0000031715.83752.a1>
- 1076 Mahapatra, S.S., Nanda, S.K., Panigrahy, B.K., 2011. A Cascaded Fuzzy Inference System for  
1077 Indian river water quality prediction. *Adv. Eng. Softw.* 42, 787–796.  
1078 <https://doi.org/10.1016/j.advengsoft.2011.05.018>
- 1079 Maier, H.R., Jain, A., Dandy, G.C., Sudheer, K.P., 2010. Methods used for the development of  
1080 neural networks for the prediction of water resource variables in river systems: Current  
1081 status and future directions. *Environ. Model. Softw.* 25, 891–909.  
1082 <https://doi.org/10.1016/j.envsoft.2010.02.003>
- 1083 Martis, R.J., Acharya, U.R., Tan, J.H., Petznick, A., Tong, L., Chua, C.K., Kwee Ng, E.Y., 2013.  
1084 Application of intrinsic Time-scale decomposition (ITD) to EEG signals for automated  
1085 seizure prediction. *Int. J. Neural Syst.* 23, 1350023.  
1086 <https://doi.org/10.1142/S0129065713500238>
- 1087 Maxwell, D.H., Jackson, B.M., McGregor, J., 2018. Constraining the ensemble Kalman filter for  
1088 improved streamflow forecasting. *J. Hydrol.* 560, 127–140.  
1089 <https://doi.org/10.1016/J.JHYDROL.2018.03.015>
- 1090 Mijares, V., Gitau, M., Johnson, D.R., 2019. A Method for Assessing and Predicting Water  
1091 Quality Status for Improved Decision-Making and Management 509–522.
- 1092 Moeeni, H., Bonakdari, H., 2017. Impact of Normalization and Input on ARMAX-ANN Model  
1093 Performance in Suspended Sediment Load Prediction. *Water Resour. Manag.* 1–19.  
1094 <https://doi.org/10.1007/s11269-017-1842-z>
- 1095 Mohammadpour, R., Shaharuddin, S., Zakaria, N.A., Ghani, A.A., Vakili, M., Chan, N.W., 2016.  
1096 Prediction of water quality index in free surface constructed wetlands. *Environ. Earth Sci.*  
1097 75, 139. <https://doi.org/10.1007/s12665-015-4905-6>

- 1098 Moradkhani, H., Sorooshian, S., Gupta, H. V., Houser, P.R., 2005. Dual state-parameter  
 1099 estimation of hydrological models using ensemble Kalman filter. *Adv. Water Resour.* 28,  
 1100 135–147. <https://doi.org/10.1016/J.ADVWATRES.2004.09.002>
- 1101 Motagh, M., Shamshiri, R., Haghshenas Haghighi, M., Wetzel, H.-U., Akbari, B., Nahavandchi,  
 1102 H., Roessner, S., Arabi, S., 2017. Quantifying groundwater exploitation induced subsidence  
 1103 in the Rafsanjan plain, southeastern Iran, using InSAR time-series and in situ  
 1104 measurements. *Eng. Geol.* 218, 134–151. <https://doi.org/10.1016/J.ENGGEOL.2017.01.011>
- 1105 Najah, A., El-Shafie, A., Karim, O.A., Jaafar, O., 2011. Integrated versus isolated scenario for  
 1106 prediction dissolved oxygen at progression of water quality monitoring stations. *Hydrol.*  
 1107 *Earth Syst. Sci.* 15, 2693–2708. <https://doi.org/10.5194/hess-15-2693-2011>
- 1108 Najah Ahmed, A., Binti Othman, F., Abdulmohsin Afan, H., Khaleel Ibrahim, R., Ming Fai, C.,  
 1109 Shabbir Hossain, M., Ehteram, M., Elshafie, A., 2019. Machine learning methods for better  
 1110 water quality prediction. *J. Hydrol.* 578, 124084.  
 1111 <https://doi.org/10.1016/j.jhydrol.2019.124084>
- 1112 Nath, B.K., Chaliha, C., Bhuyan, B., Kalita, E., Baruah, D.C., Bhagabati, A.K., 2018. GIS  
 1113 mapping-based impact assessment of groundwater contamination by arsenic and other  
 1114 heavy metal contaminants in the Brahmaputra River valley: A water quality assessment  
 1115 study. *J. Clean. Prod.* 201, 1001–1011. <https://doi.org/10.1016/j.jclepro.2018.08.084>
- 1116 Naubi, I., Zardari, N.H., Shirazi, S.M., Ibrahim, N.F.B., Baloo, L., 2016. Effectiveness of water  
 1117 quality index for monitoring Malaysian river water quality. *Polish J. Environ. Stud.* 25,  
 1118 231–239. <https://doi.org/10.15244/pjoes/60109>
- 1119 Nayak, P.C., Rao, Y.R.S., Sudheer, K.P., 2006. Groundwater Level Forecasting in a Shallow  
 1120 Aquifer Using Artificial Neural Network Approach. *Water Resour. Manag.* 20, 77–90.  
 1121 <https://doi.org/10.1007/s11269-006-4007-z>
- 1122 Nguyen Hien Than, Che Dinh Ly, Pham Van Tat, Nguyen Ngoc Thanh, 2016. Application of a  
 1123 Neural Network Technique for Prediction of the Water Quality Index in the Dong Nai  
 1124 River, Vietnam. *J. Environ. Sci. Eng. B* 5, 363–370. <https://doi.org/10.17265/2162-5263/2016.07.007>
- 1126 Ocampo-Duque, W., Ferré-Huguet, N., Domingo, J.L., Schuhmacher, M., 2006. Assessing water  
 1127 quality in rivers with fuzzy inference systems: A case study. *Environ. Int.* 32, 733–742.  
 1128 <https://doi.org/10.1016/j.envint.2006.03.009>
- 1129 Palizdan, N., Falamarzi, Y., Huang, Y.F., Lee, T.S., Ghazali, A.H., 2015. Temporal precipitation  
 1130 trend analysis at the langat river Basin, Selangor, Malaysia. *J. Earth Syst. Sci.* 124, 1623–  
 1131 1638. <https://doi.org/10.1007/s12040-015-0636-z>
- 1132 Pham, H., Rahman, M.M., Nguyen, N.C., Vo, P. Le, Van, T. Le, Ngo, H., 2017. Assessment of  
 1133 Surface Water Quality Using the Water Quality Index and Multivariate Statistical  
 1134 Techniques-A Case Study: The Upper Part of Dong Nai River Basin, Vietnam. *J. Water*  
 1135 *Sustain.* 7, 225–245. <https://doi.org/10.11912/jws.2017.7.4>
- 1136 Rezaeian-Zadeh, M., Zand-Parsa, S., Abghari, H., Zolghadr, M., Singh, V.P., 2012. Hourly air  
 1137 temperature driven using multi-layer perceptron and radial basis function networks in arid  
 1138 and semi-arid regions. *Theor. Appl. Climatol.* <https://doi.org/10.1007/s00704-012-0595-0>
- 1139 Rezaie-Balf, M., Fani Nowbandegani, S., Samadi, S.Z., Fallah, H., Alaghmand, S., 2019a. An  
 1140 Ensemble Decomposition-Based Artificial Intelligence Approach for Daily Streamflow  
 1141 Prediction. *Water* 11, 709. <https://doi.org/10.3390/w11040709>
- 1142 Rezaie-Balf, M., Kim, S., Fallah, H., Alaghmand, S., 2019b. Daily river flow forecasting using  
 1143 ensemble empirical mode decomposition based heuristic regression models: Application on

- 1144 the perennial rivers in Iran and South Korea. *J. Hydrol.* 572, 470–485.  
 1145 <https://doi.org/10.1016/j.jhydrol.2019.03.046>
- 1146 Rezaie-Balf, M., Naganna, S.R., Kisi, O., El-Shafie, A., 2019c. Enhancing streamflow  
 1147 forecasting using the augmenting ensemble procedure coupled machine learning models:  
 1148 case study of Aswan High Dam. *Hydrol. Sci. J.* 1–18.  
 1149 <https://doi.org/10.1080/02626667.2019.1661417>
- 1150 Robert K, H., 1965. An index number system for rating water quality. *ournal Water Pollut.*  
 1151 *Control Fed.* 3, 300–306.
- 1152 Roveda, S.R.M.M., Bondança, A.P.M., Silva, J.G.S., Roveda, J.A.F., Rosa, A.H., 2010.  
 1153 Development of a water quality index using a fuzzy logic: A case study for the sorocaba  
 1154 river. 2010 IEEE World Congr. Comput. Intell. WCCI 2010.  
 1155 <https://doi.org/10.1109/FUZZY.2010.5584172>
- 1156 Sahoo, M.M., Patra, K.C., Khatua, K.K., 2015. Inference of Water Quality Index Using ANFIA  
 1157 and PCA. *Aquat. Procedia* 4, 1099–1106. <https://doi.org/10.1016/j.aqpro.2015.02.139>
- 1158 Said, A., Stevens, D.K., Sehlke, G., 2004. An Innovative Index for Evaluating Water Quality in  
 1159 Streams. *Environ. Manage.* 34, 406–414. <https://doi.org/10.1007/s00267-004-0210-y>
- 1160 Sarkar, S.K., Saha, M., Takada, H., Bhattacharya, A., Mishra, P., Bhattacharya, B., 2007. Water  
 1161 quality management in the lower stretch of the river Ganges, east coast of India: an  
 1162 approach through environmental education. *J. Clean. Prod.* 15, 1559–1567.  
 1163 <https://doi.org/10.1016/j.jclepro.2006.07.030>
- 1164 Sharma, D., Lie, T.T., 2012. Wind speed forecasting using hybrid ANN-Kalman Filter  
 1165 techniques, in: 2012 10th International Power & Energy Conference (IPEC). IEEE, pp.  
 1166 644–648. <https://doi.org/10.1109/ASSCC.2012.6523344>
- 1167 Singh, J., Knapp, H.V., Arnold, J.G., Demissie, M., 2005. Hydrological modeling of the Iroquois  
 1168 River watershed using HSPF and SWAT. *J. Am. Water Resour. Assoc.* 41, 343–360.  
 1169 <https://doi.org/10.1111/j.1752-1688.2005.tb03740.x>
- 1170 Sinha, K., (Saha), P. Das, 2014. Assessment of water quality index using cluster analysis and  
 1171 artificial neural network modeling: a case study of the Hooghly River basin, West Bengal,  
 1172 India. *Desalin. Water Treat.* 54, 28–36. <https://doi.org/10.1080/19443994.2014.880379>
- 1173 Soo, E.Z.X., Jaafar, W.Z.W., Lai, S.H., Othman, F., Elshafie, A., Islam, T., Srivastava, P., Hadi,  
 1174 H.S.O., 2019. Evaluation of bias-adjusted satellite precipitation estimations for extreme  
 1175 flood events in Langat river basin, Malaysia. *Hydrol. Res.* 51, 105–126.  
 1176 <https://doi.org/10.2166/nh.2019.071>
- 1177 Suhaila, J., Deni, S.M., Zawiah Zin, W.A.N., Jemain, A.A., 2010. Trends in Peninsular Malaysia  
 1178 rainfall data during the southwest monsoon and northeast monsoon seasons: 1975-2004.  
 1179 *Sains Malaysiana* 39, 533–542.
- 1180 Tan, M.L., Samat, N., Chan, N.W., Lee, A.J., Li, C., 2019. Analysis of precipitation and  
 1181 temperature extremes over the Muda River Basin, Malaysia. *Water (Switzerland)* 11, 1–17.  
 1182 <https://doi.org/10.3390/w11020283>
- 1183 Tangang, F.T., Juneng, L., Salimun, E., Sei, K.M., Le, L.J., Muhamad, H., 2012. Climate change  
 1184 and variability over Malaysia: Gaps in science and research information. *Sains Malaysiana*  
 1185 41, 1355–1366.
- 1186 Tasneem Abbasi, Shahid A., A., 2012. Water quality indices.
- 1187 Taud, H., Mas, J.F., 2018. Multilayer Perceptron (MLP). Springer, Cham, pp. 451–455.  
 1188 [https://doi.org/10.1007/978-3-319-60801-3\\_27](https://doi.org/10.1007/978-3-319-60801-3_27)
- 1189 Tiwari, S., Babbar, R., Kaur, G., 2018. Performance Evaluation of Two ANFIS Models for

- 1190 Predicting Water Quality Index of River Satluj (India). *Adv. Civ. Eng.* 2018, 1–10.  
1191 <https://doi.org/10.1155/2018/8971079>
- 1192 Wang, Z., 2018. Hourly Solar Radiation Forecasting Using a Volterra-Least Squares Support  
1193 Vector Machine Model Combined with Signal Decomposition. *Energies* 11, 68.  
1194 <https://doi.org/10.3390/en11010068>
- 1195 Wu, Z., Wang, X., Chen, Y., Cai, Y., Deng, J., 2018. Assessing river water quality using water  
1196 quality index in Lake Taihu Basin, China. *Sci. Total Environ.* 612, 914–922.  
1197 <https://doi.org/10.1016/j.scitotenv.2017.08.293>
- 1198 Yahya, A.S.A., Ahmed, A.N., Othman, F.B., Ibrahim, R.K., Afan, H.A., El-Shafie, A., Fai,  
1199 C.M., Hossain, M.S., Ehteram, M., Elshafie, A., 2019. Water quality prediction model  
1200 based support vector machine model for ungauged river catchment under dual scenarios.  
1201 *Water (Switzerland)* 11. <https://doi.org/10.3390/w11061231>
- 1202 Yaseen, Z.M., Ramal, M.M., Diop, L., Jaafar, O., Demir, V., Kisi, O., 2018. Hybrid Adaptive  
1203 Neuro-Fuzzy Models for Water Quality Index Estimation. *Water Resour. Manag.* 32, 2227–  
1204 2245. <https://doi.org/10.1007/s11269-018-1915-7>
- 1205 Yilma, M., Kiflie, Z., Windsperger, A., Gessese, N., 2018. Application of artificial neural  
1206 network in water quality index prediction: a case study in Little Akaki River, Addis Ababa,  
1207 Ethiopia. *Model. Earth Syst. Environ.* 0, 0. <https://doi.org/10.1007/s40808-018-0437-x>
- 1208 Yu, C., Li, Y., Zhang, M., 2017. Comparative study on three new hybrid models using Elman  
1209 Neural Network and Empirical Mode Decomposition based technologies improved by  
1210 Singular Spectrum Analysis for hour-ahead wind speed forecasting. *Energy Convers.*  
1211 *Manag.* 147, 75–85. <https://doi.org/10.1016/j.enconman.2017.05.008>
- 1212 Zhang, Q., Li, Z., 2019. Development of an interval quadratic programming water quality  
1213 management model and its solution algorithms. *J. Clean. Prod.* 119319.  
1214 <https://doi.org/10.1016/j.jclepro.2019.119319>
- 1215 Zhang, X., Zhang, Q., Zhang, G., Nie, Z., Gui, Z., Que, H., Zhang, X., Zhang, Q., Zhang, G.,  
1216 Nie, Z., Gui, Z., Que, H., 2018. A Novel Hybrid Data-Driven Model for Daily Land Surface  
1217 Temperature Forecasting Using Long Short-Term Memory Neural Network Based on  
1218 Ensemble Empirical Mode Decomposition. *Int. J. Environ. Res. Public Health* 15, 1032.  
1219 <https://doi.org/10.3390/ijerph15051032>
- 1220 Zhou, Y., Chang, F.-J., Guo, S., Ba, H., He, S., 2017. A robust recurrent ANFIS for modeling  
1221 multi-step-ahead flood forecast of Three Gorges Reservoir in the Yangtze River. *Hydrol.*  
1222 *Earth Syst. Sci. Discuss.* 1–29. <https://doi.org/10.5194/hess-2017-457>  
1223  
1224

1 **Highlight**

2

3 As a comprehensive review, pH and DO were the most influential parameters for WQI  
4 prediction.

5 Ensemble Kalman Filter as the DA technique is applied to generate an accurate state estimation.

6 For improving the physicochemical data to noise ratio, ITD approach hybridized with EnKF-  
7 ANN.

8 The new ITD-EnKF-ANN generally outperformed other standalone and hybrid DDMs for the  
9 prediction of WQI.

**Credit Author Statement**

**Mohammad Rezaie-Balf:** Conceptualization, Software, Supervision.

**Nasrin Fathollahzadeh Attar:** Methodology, Writing- Original draft preparation.

**Ardashir Mohammadzadeh:** Software, Methodology.

**Muhammad Ary Murti:** Resources, Writing- Original draft preparation.

**Ali Najah Ahmed:** Writing- Reviewing and Editing.

**Chow Ming Fai:** Resources, Writing- Original draft preparation.

**Narjes Nabipour:** Writing and Reviewing, Formal analysis.

**Sina Alaghmand:** Writing- Reviewing and Editing.

**Ahmed El-Shafie:** Visualization, Supervision.

**Declaration of interests**

The authors declare that they have no known competing financial interests or personal relationships that could have appeared to influence the work reported in this paper.

The authors declare the following financial interests/personal relationships which may be considered as potential competing interests: